OsHAD1, a Haloacid Dehalogenase-Like APase, Enhances Phosphate Accumulation[1]

Bipin K. Pandey,[2] Poonam Mehra,[2] Lokesh Verma, Jyoti Bhadouria, and Jitender Giri[3]

National Institute of Plant Genome Research, Aruna Asaf Ali Marg, New Delhi-110067, India

ORCID ID: 0000-0001-6969-5187 (J.G.).

Phosphorus (P) deficiency limits plant growth and yield. Since plants can absorb only the inorganic form of P (Pi), a large portion of soil P (organic and inorganic P complexes) remains unused. Here, we identified and characterized a PHR2-regulated, novel low-Pi-responsive haloacid dehalogenase (HAD)-like hydrolase, *OsHAD1*. While OsHAD1 is a functional HAD protein having both acid phosphatase and phytase activities, it showed little homology with other known low-Pi-responsive HAD superfamily members. Recombinant OsHAD1 is active at acidic pH and dephosphorylates a broad range of organic and inorganic P-containing substrates, including phosphorylated serine and sodium phytate. Exogenous application of recombinant OsHAD1 protein in growth medium supplemented with phytate led to marked increases in growth and total P content of Pi-deficient wild-type rice (*Oryza sativa*) seedlings. Furthermore, overexpression of *OsHAD1* in rice resulted in enhanced phosphatase activity, biomass, and total and soluble P contents in Pi-deficient transgenic seedlings treated with phytate as a restricted Pi source. Gene expression and metabolite profiling revealed enhanced Pi starvation responses, such as up-regulation of multiple genes involved in Pi uptake and solubilization, accumulation of organic acids, enhanced secretory phosphatase activity, and depletion of ATP in overexpression lines as compared with the wild type. To elucidate the underlying regulatory mechanisms of OsHAD1, we performed in vitro pull-down assays, which revealed the association of OsHAD1 with protein kinases such as OsNDPKs. We conclude that, besides dephosphorylation of cellular organic P, OsHAD1 in coordination with kinases may regulate the phosphorylation status of downstream targets to accomplish Pi homeostasis under limited Pi supply.

Rice (*Oryza sativa*) is one of the most consumed cereals in the world. Therefore, to sustain a growing population, especially in rice-consuming areas, it is necessary to increase crop yield in coming years (Papademetriou, 2000; Tilman et al., 2011). Phosphorus (P) is an essential macronutrient for plant growth and development. It is an integral part of nucleic acids, phospholipid membranes, and many metabolic pathways. Essentially, most of the signal transduction pathways are regulated by phosphorylation and dephosphorylation events. Widespread soil inorganic phosphate (Pi) deficiency is known to limit rice yield, particularly in upland acidic soils (Kirk et al., 1998). Since most of the modern nutrient-exhaustive high-yielding rice varieties are low Pi sensitive (Wissuwa and Ae, 2001; Mehra et al., 2015, 2016), it is imperative to develop Pi-efficient high-yielding rice varieties to accomplish high rice production and reduce extensive application of phosphate fertilizers. Notably, unrestrained use of Pi fertilizers has serious ecological impacts, such as heavy metal contamination of soils (Chien et al., 2011) and eutrophication of water bodies through soil erosion or surface runoff (Ha and Tran, 2014). Additionally, fast-depleting Pi fertilizer sources (high-quality rock phosphate) are finite and nonrenewable in nature (Cordell and Neset, 2014). Therefore, improvement of the Pi use efficiency of rice could be an efficient and sustainable means for crop production.

Roots absorb P in the form of Pi from soil solution. Unfortunately, ~80% of the applied Pi fertilizers are rapidly fixed in the soil in organic/inorganic insoluble complexes due to microbial assimilation and adsorption. Therefore, up to 65% of the total soil P exists in the organic form (Harrison, 1987), which needs mineralization before root uptake (Dobermann et al., 1998). To release Pi from these bound sources, plants produce several intracellular and extracellular acid phosphatases (APases), secrete organic acids into the rhizosphere, undergo symbiotic associations with mycorrhizal fungi, and develop specialized proteoid roots (Raghothama, 1999). Among these strategies, the production of extracellular and intracellular APases is important, as these enzymes can hydrolyze a broad range of organic P sources to release Pi under low-Pi conditions. Intracellular APases maintain internal Pi homeostasis by releasing Pi from organic P compounds in the cytoplasm and vacuole, whereas extracellular APases hydrolyze organic P sources present in the extracellular matrix (Tran et al.,

[1] This work was supported by DBT (grant no. BT/PR3299/AGR/2/813/2011), Government of India, and by NIPGR core grants.

[2] These authors contributed equally to the article.

[3] Address correspondence to jitender@nipgr.ac.in.

The author responsible for distribution of materials integral to the findings presented in this article in accordance with the policy described in the Instructions for Authors (www.plantphysiol.org) is: Jitender Giri (jitender@nipgr.ac.in).

J.G. conceived original research plans and designed and supervised experiments; B.K.P. and P.M. designed and performed experiments; L.V. and J.B. performed experiments; B.K.P., P.M., and J.G. analyzed data and wrote the article.

www.plantphysiol.org/cgi/doi/10.1104/pp.17.00571

2010a). Various strategies have been employed to enhance Pi availability from organic resources by engineering phytases and APases from microbial or plant origin (Richardson et al., 2001; Zimmermann et al., 2003; Lung et al., 2005; George et al., 2007; Liu et al., 2012; Ma et al., 2012; Singh and Satyanarayana, 2012; Mehra et al., 2017). While a growing body of literature emphasizes the roles of extracellular phytases and APases in P solubilization and acquisition, the potential of intracellular phytases/APases in low-Pi tolerance has remained unrecognized.

APases such as haloacid dehalogenase (HAD) superfamily members are regulated by Pi deficiency (Baldwin et al., 2001; Hur et al., 2007; May et al., 2011). The HAD superfamily of enzymes is composed of several ATPases, epoxide hydrolases, dehalogenases, phosphonatases, phosphomutases, phosphoserine, and other phosphatases (Burroughs et al., 2006; Kuznetsova et al., 2006). *LePS2* was the first low-Pi-inducible HAD superfamily gene characterized in tomato (*Solanum lycopersicum*; Baldwin et al., 2001, 2008). The protein phosphatase activity of overexpressed LePS2 led to increased APase activity, anthocyanin accumulation, and delayed flowering in tomato (Baldwin et al., 2008). Similarly, another *HAD* gene, *PvHAD1*, showed low-Pi-specific induction and encodes a functional Ser/Thr phosphatase (Liu et al., 2010). In Arabidopsis (*Arabidopsis thaliana*), two low-Pi-responsive HADs, *AtPPsPase1* and *AtPECP1*, were reported to encode functional pyrophosphatase and phosphoethanolamine phosphatase, respectively (May et al., 2011, 2012). Later, PvPS2:1, a plasma membrane-localized homolog of LePS2, was reported to increase Pi acquisition and root growth in Arabidopsis overexpressing transgenics (Liang et al., 2012). These studies suggest the important functions of HAD superfamily members in regulating Pi homeostasis. In rice, only one *HAD*, *OsACP1* (also a homolog of *LePS2*), was shown to be up-regulated under Pi deficiency (Hur et al., 2007). However, the physiological roles of any other HAD are largely unknown in rice. Therefore, in this study, we identified and characterized a novel low-Pi-inducible HAD gene, *OsHAD1*, in rice. Biochemical assays revealed that OsHAD1 is a functional APase with broad substrate specificities and possesses substantial protein phosphatase and phytase activities. Furthermore, overexpression of *OsHAD1* led to increased APase/phytase activity, P accumulation, and improved growth of rice under restricted Pi supply. Here, to our knowledge for the first time, we provide a detailed investigation on a HAD superfamily member in rice and its efficacy in improving Pi homeostasis.

RESULTS

OsHAD1 Is Induced under Pi Deficiency

We earlier identified several low-Pi-responsive genes using a comparative transcriptomic approach in low-Pi-tolerant and -sensitive rice genotypes (Mehra et al., 2016). Among these, a HAD (Os03g61829), designated here as *OsHAD1*, was found to be differentially induced in root and shoot under low Pi. *OsHAD1* was highly up-regulated in the low-Pi-tolerant genotype Dular as compared with PB1, a low-Pi-sensitive modern high-yielding genotype. To further assess the low Pi responsiveness of *OsHAD1*, gene expression was analyzed after 5, 15, and 21 d of Pi deficiency. We found increased transcript levels of *OsHAD1* with increasing duration of low-Pi stress, preferentially in shoot (Fig. 1A). Notably, up-regulation of *OsHAD1* was higher in Dular as compared with PB1, except at 5 d. Furthermore, *OsHAD1* showed significant up-regulation in P, K, and Fe deficiencies at 7 d of stress treatment. However, after prolonged stress exposure for 15 d, *OsHAD1* was specifically up-regulated only in low Pi (Fig. 1B). Additionally, expression analysis of *OsHAD1* at different developmental stages and tissues showed that it is expressed in almost all organs to varying levels (Supplemental Fig. S1). *OsHAD1* expression was higher in shoot and floral organs. These results revealed that *OsHAD1* is low-Pi responsive, with preferential expression in shoot and floral organs.

OsPHR2 Regulates the Expression of *OsHAD1*

The PHR1 transcription factor is a central regulator of low-Pi-responsive genes in various plants. OsPHR2 is a functional ortholog of AtPHR1 (Zhou et al., 2008). We found three P1BS (PHR2-binding site) elements at positions −864, −765, and −442 in a 2-kb promoter region of *OsHAD1* (Fig. 1C). Our electrophoretic mobility shift assay showed that OsPHR2 binds physically to the *OsHAD1* promoter (Fig. 1C). Furthermore, this interaction was reduced significantly when a 100× excess of unlabeled *OsHAD1* promoter probe was used as a competitive inhibitor. All this confirmed that *OsHAD1* is a component of the rice low-Pi-responsive machinery regulated by OsPHR2.

OsHAD1 Is a Novel Functional Acid Phosphatase

Protein sequence alignment revealed the divergence of OsHAD1 from other known plant HAD domain-containing proteins (Fig. 2A). However, as expected for the HAD family, homology was restricted to strictly conserved residues only (Fig. 2B). Furthermore, OsHAD1 contains four conserved motifs (DxDxT/V, S/T, K, and DD) in which the first motif (DxDxT/V) is essential for APase activity (Fig. 2B). It is reported that the first Asp residue of the first conserved motif (D^1LD^2DT) acts as a nucleophile and that the second Asp residue acts as acid or base, which protonates the leaving groups in most of the phosphatases from the HAD superfamily (Burroughs et al., 2006). Thus, this motif can play an important role in releasing Pi from various P-containing compounds.

To test whether *OsHAD1* encodes an active protein, we purified recombinant OsHAD1 protein with a 6xHis tag from *Escherichia coli* (Supplemental Fig. S2). Purified recombinant OsHAD1 showed phosphatase activity with

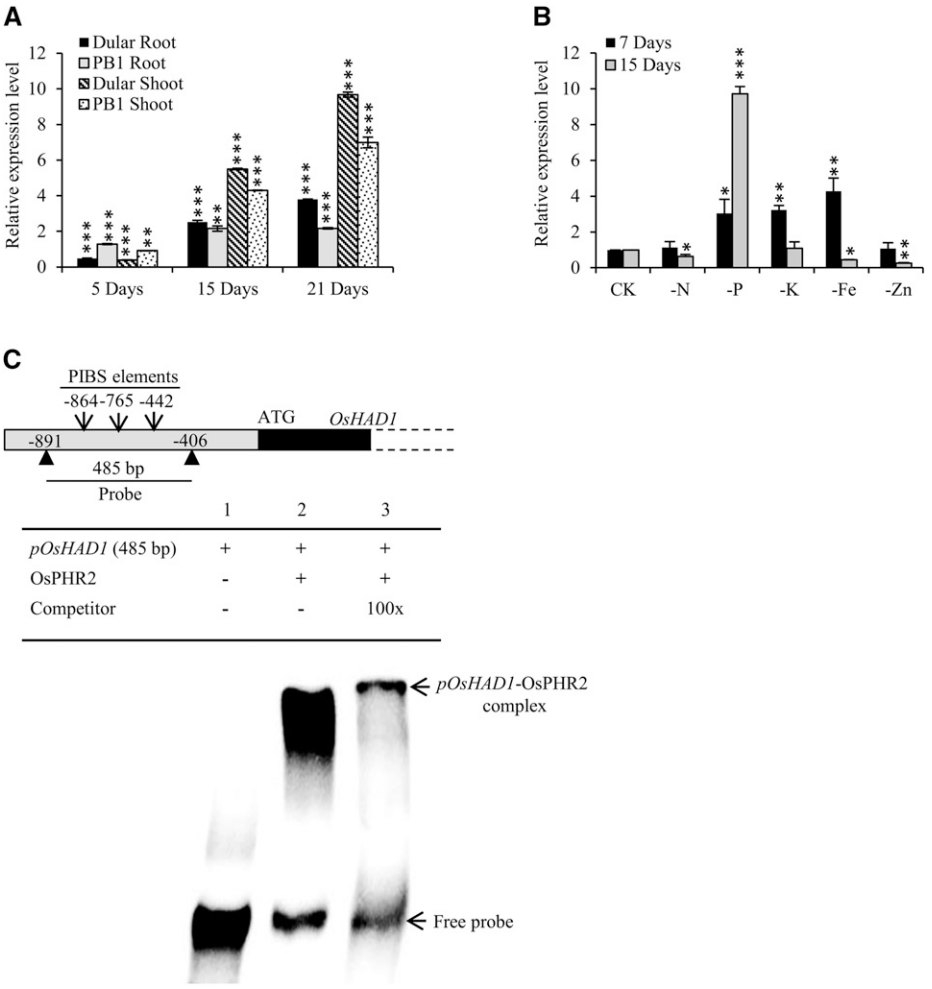

Figure 1. Transcriptional regulation of *OsHAD1*. A, Relative expression of *OsHAD1* in Dular and PB1 roots and shoot under Pi-deficient (1 μM) conditions with respect to corresponding Pi-sufficient (320 μM) conditions at 5, 15, and 21 d. B, Relative expression of *OsHAD1* under N-, P-, K-, Fe-, and Zn-deficient conditions in roots after 7 and 15 d of the respective deficiency treatments. Relative expression levels under deficient conditions were calculated with respect to expression levels under the sufficient nutrient supply condition (CK). Expression profiling was carried out with qRT-PCR. Significant differences between deficient versus sufficient treatments were evaluated by Student's *t* test. Asterisks indicate $P \leq 0.05$ (*), $P \leq 0.01$ (**), and $P \leq 0.001$ (***). C, Electrophoretic mobility shift assay showing physical binding of OsPHR2 with the *OsHAD1* promoter. A 485-bp radiolabeled promoter of *OsHAD1* (*pOsHAD1*) containing three P1BS cis-elements at −864, −765, and −442 bp was used as a probe. Lane 1, Radiolabeled free promoter probe of *OsHAD1* (12.74 ng); lane 2, [α-^{32}P]CTP-labeled probe of *OsHAD1* (12.74 ng) plus OsPHR2 protein (1.5 μg); lane 3, OsPHR2 protein (1.5 μg) plus labeled promoter probe of *OsHAD1* (12.74 ng) and a 100-fold excess of unlabeled *OsHAD1* probe as a competitive inhibitor.

pNPP as a substrate. We next used various other P-containing substrates to elucidate the substrate specificity of OsHAD1 (Table I). This assay showed that free nucleotides like ATP, ADP, and AMP are the preferred substrates of OsHAD1. However, OsHAD1 also exhibited moderate phosphatase activity with sodium phytate, Glc-6-P, Fru-6-P, Rib-5-P, and other P-containing compounds (Table I). Maximum phosphatase activity was obtained with ATP (40.2%) as compared with pNPP (100%). Notably, OsHAD1 also was able to hydrolyze phosphorylated Ser and, to some extent, phosphorylated Tyr. These results confirmed the protein phosphatase activity of OsHAD1.

A pH kinetics study revealed that OsHAD1 is an APase, as it could hydrolyze substrates (pNPP, ATP, AMP, and Rib-5-P) at very low pH 2 to 5 (Fig. 2C). OsHAD1 was found to be moderately thermostable (25°C–55°C), with maximum phosphatase activity at 37°C (Fig. 2D). Furthermore, different metal ions could enhance the OsHAD1 activity ($Mg^{2+} > Ni^{2+} > Co^{2+} > Mn^{2+}$); Mg^{2+} turned out to be the preferential cofactor. High Pi concentrations, Cd^{2+}, citrate, EDTA, and Ca^{2+}, seemed to be inhibitors of OsHAD1 phosphatase activity (Fig. 2E). Furthermore, OsHAD1 showed specific activity: 334.47, 6.95, and 0.687 μmol P released min^{-1} mg^{-1} protein with pNPP, ATP, and sodium phytate, respectively. Lastly, OsHAD1 showed higher affinity (K_m = 0.5 and 0.58 mM) with pNPP and sodium phytate and lower affinity with ATP (K_m = 1.42 mM; Fig. 2F).

Site-Directed Mutagenesis Revealed That Asp Residues Are Critical for OsHAD1 Activity

To confirm the role of motif 1, which is critical for phosphatase activity, we independently modified two key Asp residues, D^{16} and D^{18}, to Ala from motif I ($D^{16}LD^{18}DT$) of OsHAD1 (Fig. 2B). Notably, these mutations (D16A and D18A) led to the absolute loss of phosphatase activity in OsHAD1 (Fig. 2G). These results confirmed the importance of Asp residues for the catalytic activity of OsHAD1.

Exogenous Application of OsHAD1 Enhances the Growth of Pi-Deficient Plants on Phytate-Supplemented Medium

To measure the impact of phytase activity of OsHAD1, 15-d-old Pi-starved seedlings were supplemented with

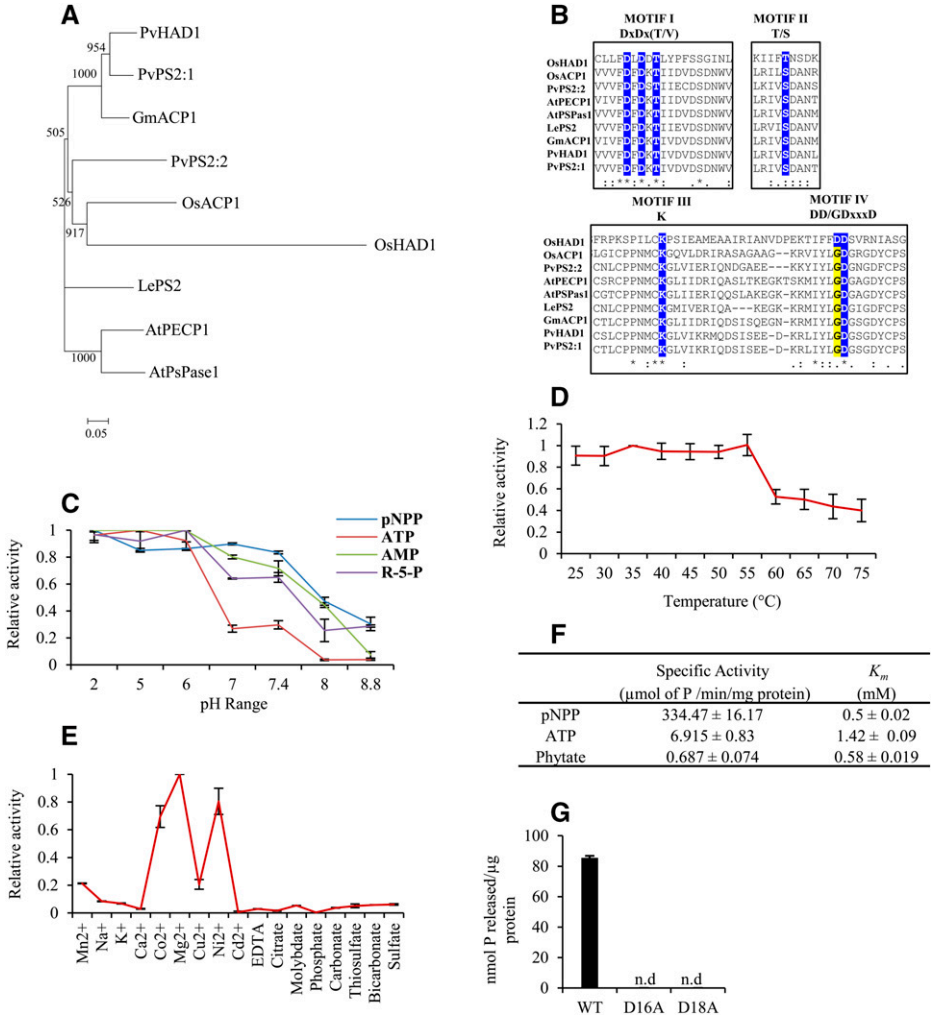

	Specific Activity (μmol of P /min/mg protein)	K_m (mM)
pNPP	334.47 ± 16.17	0.5 ± 0.02
ATP	6.915 ± 0.83	1.42 ± 0.09
Phytate	0.687 ± 0.074	0.58 ± 0.019

Figure 2. Phylogenetic relationships and biochemical properties of OsHAD1. A, Phylogenetic relationships of OsHAD1 with known HAD proteins from rice (OsACP1), Arabidopsis (AtPsPase1 and AtPECP1), tomato (LePS2), soybean (*Glycine max*; GmACP1), and common bean (*Phaseolus vulgaris*; PvHAD1, PvPS2:1, and PvPS2:2), shown by a neighbor-joining phylogenetic tree. The scale bar represents the rate of amino acid substitutions. Bootstrap values are mentioned at the branches. B, Alignment of the amino acid sequence of OsHAD1 with protein sequences of LePS2, OsACP1, PvPS2:1, PvPS2:2, AtPECP1, AtPsPase1, GmACP1, and PvHAD1. Conserved HAD motifs (I–IV) are highlighted. C, Effects of different pH values on the activity of OsHAD1 using 10 mM pNPP, ATP, AMP, and Rib-5-P (R-5-P) as substrates in sodium acetate buffer (pH range 2–6) and Tris-Cl buffer (pH range 7–8.8). D, Relative activity of OsHAD1 at different temperatures. E, Effects of different activators and inhibitors on the activity of OsHAD1. F, Specific activity and K_m values of OsHAD1 with pNPP, ATP, and sodium phytate as substrates. G, Phosphatase activity of wild-type (unmutated; WT) and mutated (D16A and D18A) OsHAD1 recombinant proteins. n.d. indicates no activity detection. Relative activity was calculated with respect to the highest activity, which was taken as 1. Error bars in all graphs indicate SD from three independent measurements.

100 μM sodium phytate with or without 125 ng mL^{-1} recombinant OsHAD1 in Yoshida medium for 7 d. The overall growth of phytate + OsHAD1-supplemented plants was superior to that of plants supplemented with phytate only (Fig. 3A). Fresh root and shoot biomass of phytate + OsHAD1-supplied plants was increased up to 58.8% and 31.2%, respectively, as compared with phytate-supplemented plants (Fig. 3, D and E). Increased shoot biomass was in good concordance with the increased number of tillers and leaf numbers of phytate + OsHAD1-supplemented plants (Fig. 3, B and C). Similar trends also were observed in dry biomass gain (Fig. 3, F and G). To understand the reason for the enhanced growth after exogenous application of OsHAD1, we quantified the total P content of root and shoot separately. Phytate + OsHAD1-supplied plants showed significantly higher P content (120% in roots and 33% in shoots) as compared with phytate-supplemented plants (Fig. 3, H and I). Moreover, exogenous application of a mutagenized protein of OsHAD1 (D16A) in phytate-supplemented medium resulted in no significant growth advantage to wild-type seedlings as compared with Pi-deficient seedlings treated with phytate alone (Supplemental Fig. S3). Overall, these results showed the efficacy of

Table I. *Relative activity of recombinant OsHAD1 with different organic and inorganic P compounds*

Relative percentage activity was calculated with respect to the activity with pNPP as substrate.

Substrate	Percentage Activity
pNPP	100.00
ATP	40.20
ADP	17.28
AMP	25.21
Inorganic pyrophosphate	2.69
Phytic acid	1.70
O-Phosphoserine	2.29
O-Phosphothreonine	0.96
Glc-6-P	6.23
Fru-6-P	4.14
Man-6-P	4.73
Rib-5-P	10.48
dRib-5-P	6.26
α-D-Man-1-P	3.68

OsHAD1 in the solubilization of phytate and, thus, improved plant growth.

Overexpression of *OsHAD1* Enhances Pi Accumulation in Transgenic Rice

Our results so far revealed OsHAD1 as a low-Pi-responsive APase with broad substrate specificities. Therefore, to study the effect of its phosphatase activity on low-Pi tolerance, we cloned *OsHAD1* under the control of a constitutive promoter (*ZmUbi1*) and raised overexpression lines of *OsHAD1* in rice. Five homozygous lines were used for the initial screening, and the three highest overexpressing (OE) lines were selected for further study. Transgenics were confirmed for gene integration and overexpression using PCR, qRT-PCR, western blotting, and GUS histochemical assay (Supplemental Fig. S4). Immunoblotting of total plant protein with anti-OsHAD1 antibody confirmed the overexpression of OsHAD1 in all three OE lines; however, no band was detected in wild-type seedlings, indicating very low expression of OsHAD1 under the native condition (Supplemental Fig. S4B). To test low-Pi tolerance of OE lines, we grew OE lines along with the wild type under Pi-deficient (−P; 1 μM NaH_2PO_4) and Pi-sufficient (+P; 320 μM NaH_2PO_4) conditions for 30 d (Fig. 4, A and B). Additionally, we treated 15-d-old Pi-deficient wild-type and transgenic lines with 100 μM phytate (+Phytate) as a restricted P source for the next 15 d (Fig. 4C). Interestingly, dry root and shoot biomass of *OsHAD1* overexpressed lines increased significantly (48.5% and 68.8%, respectively) as compared with the wild type under phytate treatment (Fig. 4, D and E). Similarly, the root biomass of OE1 and OE8 was significantly higher (18.5% and 25.9%, respectively) than in the wild type under Pi deficiency (Fig. 4D). Furthermore, total P content was significantly higher in OE lines under Pi-sufficient and phytate recovery conditions in root and shoot (Fig. 4, F and G). However, under Pi deficiency, none of the lines showed significant change in P accumulation, as a very low amount of Pi was supplied. Intriguingly, transgenics grown under Pi-sufficient conditions showed some growth retardation, which could be due to high P accumulation.

We further extended our analysis to wild-type and *OsHAD1* transgenic plants raised in a soil system using PVC pipes filled with sand, soilrite, and vermiculite (Supplemental Fig. S5). Atomic absorption spectroscopy measurements showed that a formulated mixture had a very low amount of P (0.1 μM). These pipes were supplied with Pi-sufficient, Pi-deficient, and phytate-containing growth media (see "Materials and Methods"). Notably, phytate-supplemented OE lines had significantly higher shoot biomass (15%–40%) as compared with the wild type (Supplemental Fig. S6B). Furthermore, Pi-deficient plants also showed 38% more shoot biomass as compared with controls (Supplemental Fig. S6B). Total P in all the OE lines was significantly higher in both root and shoot than in the wild type under +P and phytate treatments (Supplemental Fig. S6, C and D). Moreover, a significant increase in total P also was found in shoot of *OsHAD1* OE lines under the Pi-deficient condition (Supplemental Fig. S6D). These results confirmed that overexpression of *OsHAD1* leads to increased P accumulation in plants under both hydroponics and soil conditions.

Similar to hydroponics, growth retardation also was seen in overexpression lines in the soil system as compared with wild-type plants under high-Pi conditions. To investigate this further, we performed a dose-dependent experiment consisting of different Pi concentrations (16, 32, 160, and 320 μM) for 50 d in soil. Although the biomass of *OsHAD1* OE lines was significantly higher at 32 μM Pi as compared with the wild type (Fig. 5B), the same was significantly decreased at higher dosages of Pi (160 and 320 μM) than in the wild type (Fig. 5, C and D). Consistent with previous observations, total P content of *OsHAD1* OE lines was significantly higher at all concentrations of external Pi as compared with wild-type plants (Fig. 5). To this end, we conclude that *OsHAD1* overexpression led to increased P accumulation in rice and that transgenics perform better in low-Pi conditions.

OsHAD1 Is a Cytosolic and Membrane-Localized Protein

It is possible that OsHAD1 is a secretory APase and hydrolyzes external Pi compounds in the rhizosphere of transgenics. Therefore, we studied its subcellular localization using an OsHAD1:YFP fusion protein to determine its secretory or nonsecretory nature. OsHAD1:YFP was found to be localized in cytosol and either cell wall or plasma membrane in onion (*Allium cepa*) and *Nicotiana benthamiana* epidermal cells (Supplemental Figs. S7A and S8A). Interestingly, plasmolysis of *OsHAD1*-overexpressing cells confirmed that OsHAD1 is a cytosolic protein and, therefore, an intracellular or nonsecretory APase (Supplemental Figs. S7B and S8B).

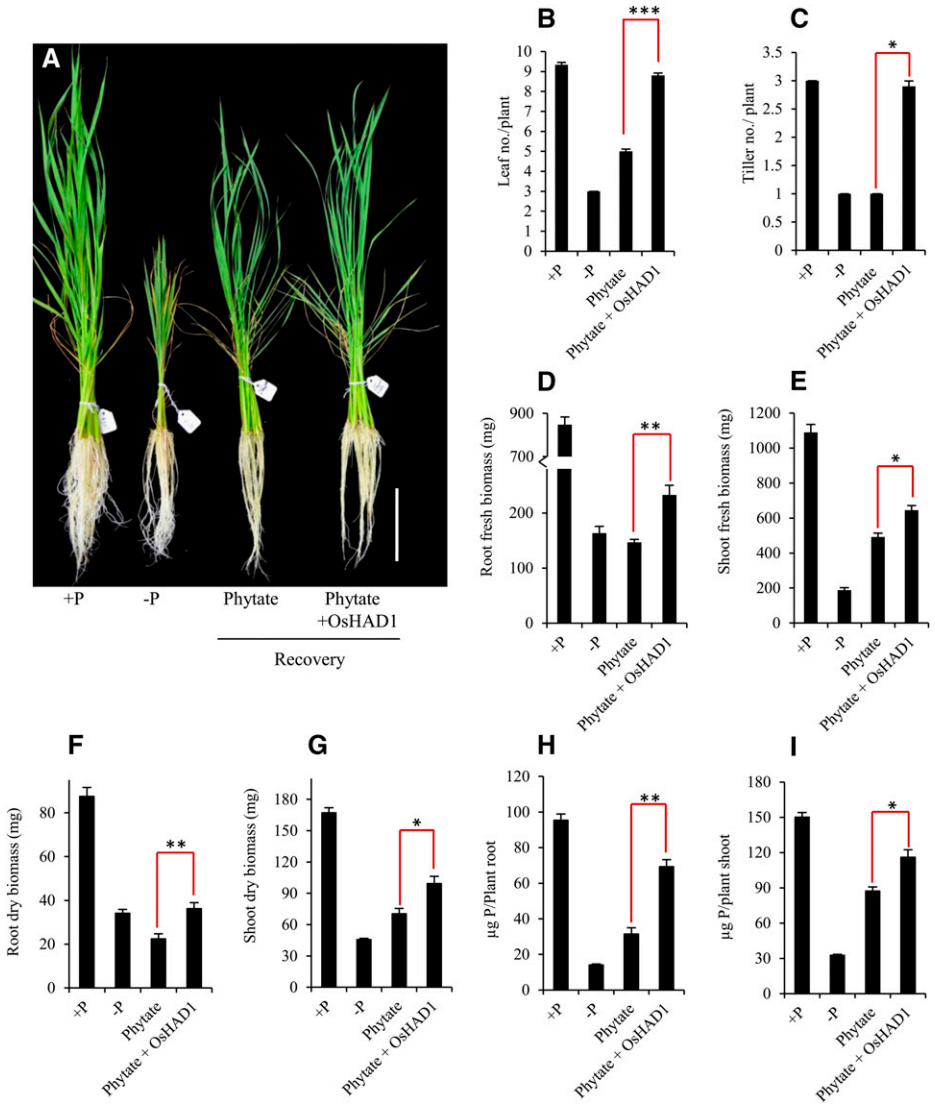

Figure 3. Effects of exogenously supplied OsHAD1 with phytate on the growth of Pi-starved wild-type rice plants. A, Improvement in growth of 15-d-old Pi-deficient wild-type rice seedlings after 7 d of recovery with phytate (100 μM) or phytate + OsHAD1 (125 ng of OsHAD1 per 1 mL of Yoshida medium supplemented with 100 μM phytate). Each stack consists of five seedlings. Bar = 10 cm. B to I, Leaf number (B), tiller number (C), fresh root biomass (mg plant^{-1}; D), fresh shoot biomass (mg plant^{-1}; E), root dry biomass (F), shoot dry biomass (G), and total P content (μg plant shoot^{-1}; H) in dried shoot as well as total P content (μg plant root^{-1}; I) in dried roots of wild-type rice seedlings grown under Pi sufficient (+P), Pi deficient (−P), phytate recovered (Phytate), and phytate plus OsHAD1 (Phytate+OsHAD1) recovered conditions. –P and +P plants were provided 1 μM Pi (NaH_2PO_4) and 320 μM Pi, respectively, for 22 d in Yoshida medium. Error bars indicate SE (n = 20). Student's t test was used to calculate significance. Asterisks indicate $P \leq 0.05$ (*), $P \leq 0.01$ (**), and $P \leq 0.001$ (***).

OsHAD1 Overexpressed Lines Showed Increased APase Activity and Soluble P Content

Since OsHAD1 is an intracellular APase, we tested its activity in 30-d-old hydroponically raised OE lines. Enhanced intracellular APase activity would increase Pi levels in a cell system. We found significantly increased phosphatase activity in roots and shoots of OE lines as compared with the wild type (Fig. 6, A and B). Notably, OE lines also showed significantly higher phytase activity under phytate-supplied conditions (Supplemental Fig. S9).

To further validate the consequence of elevated intracellular APase activity (Pi solubilization from cellular organic P compounds) in OE lines, Pi content was measured temporally in +P seedlings transferred to −P or phytate-supplemented medium. Transgenics showed higher soluble Pi content than the wild type under both conditions (Fig. 6, C and D). This indicates that enhanced cellular Pi levels in *OsHAD1* OE lines could be due to increased intracellular APase activity.

Increased Accumulation of P in *OsHAD1* OE Lines Is Mediated by an Enhanced Phosphate Starvation Response

Increased Expression of Pi Transporters and Secretory APases in OE Lines

Next, we studied the expression patterns of phosphate starvation response (PSR) Pi transporters (*OsPT1*, *OsPT2*, *OsPT4*, *OsPT6*, *OsPT8*, and *OsPT9*) to determine the reason for the greater P accumulation in transgenics. Notably, *OsPT8*, *OsPT2*, *OsPT9*, and *OsPT1* were significantly up-regulated in roots of *OsHAD1* plants under the +P condition as compared with the wild type. Their expression was further induced under −P with higher magnitude in OE1 (Fig. 7). Interestingly, *OsPT4* and *OsPT6* were highly up-regulated in overexpressed lines under −P as compared with the wild type (Fig. 7, C and D). We further determined the expression of several predicted secretory phytases and low-P-responsive purple acid phosphatases (PAPs) in

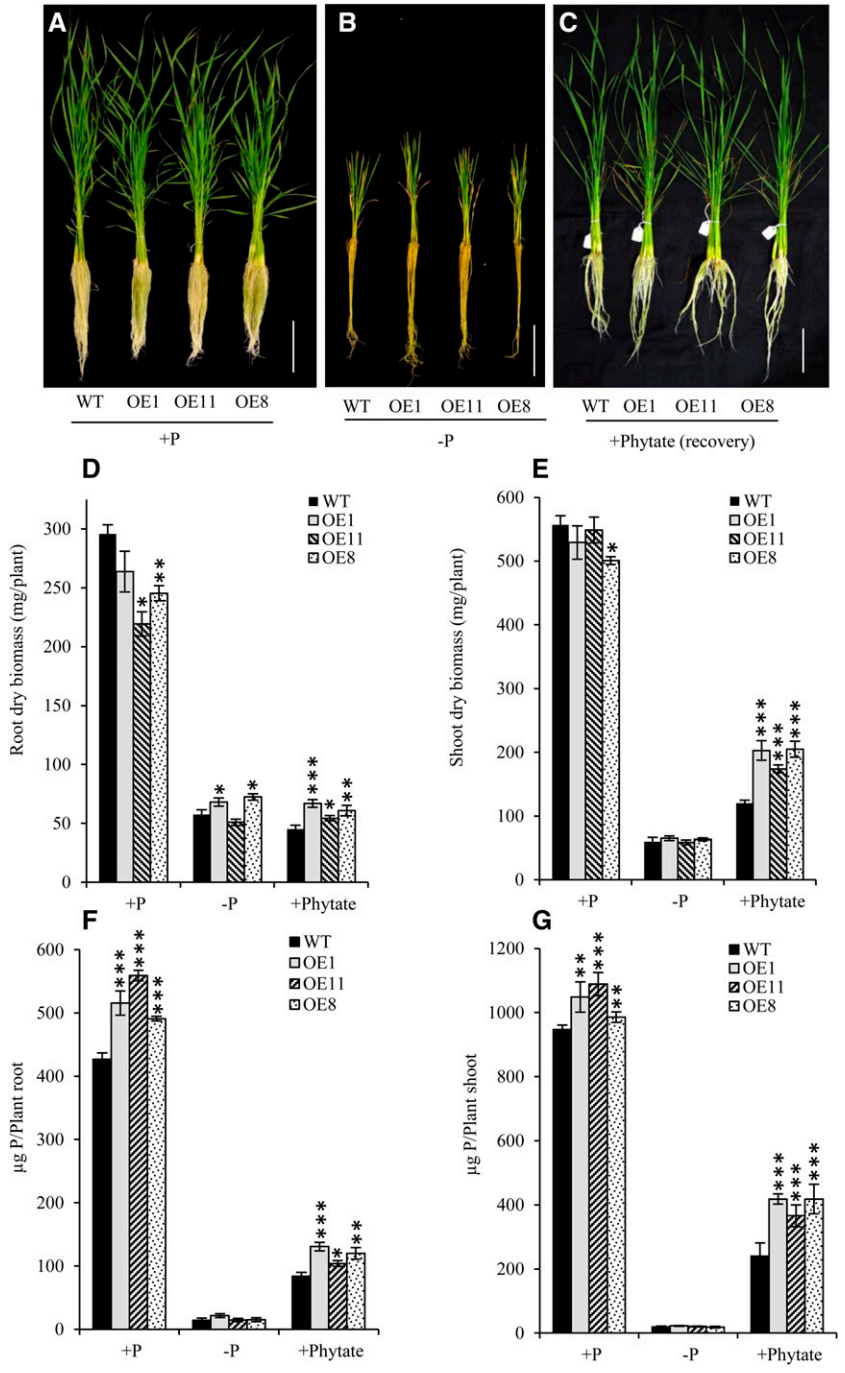

Figure 4. Effects of *OsHAD1* overexpression on biomass and total P content in hydroponics. A to C, Plant phenotypes are shown for 30-d-old hydroponically raised wild-type (WT) and *OsHAD1* overexpressed lines (OE1, OE11, and OE8) grown under 320 μM Pi (+P) for 30 d (A), 1 μM Pi (−P) for 30 d (B), or 1 μM Pi (−P) for 15 d followed by recovery with 100 μM phytate (+Phytate) for another 15 d (C). Each stack consists of three seedlings. Bars = 10 cm. D to G, Dry root biomass (D), dry shoot biomass (E), total P content per plant root (F), and total P content per plant shoot (G) of wild-type and *OsHAD1* overexpression lines under control conditions (+P; 30 d), Pi deficiency (−P; 30 d), and phytate recovery (15 d of −P treatment followed by recovery with 100 μM phytate for another 15 d). Error bars in all graphs indicate SE (n = 10). Significant differences in overexpression lines with respect to the wild type were determined by Student's t test. Asterisks indicate $P \leq 0.05$ (*), $P \leq 0.01$ (**), and $P \leq 0.001$ (***).

30-d-old hydroponically raised wild-type and OE lines. Interestingly, most of the phosphatases were consistently up-regulated in OE lines as compared with the wild type (Fig. 7G). In concordance with this, overexpression of *OsHAD1* led to increased secretory APase activity as compared with the wild type (Supplemental Fig. S10). Therefore, the increased growth and P accumulation in transgenics could be additive effects of enhanced hydrolysis of cellular Pi, activity of Pi transporters, and secretory phosphatases/phytases.

OsHAD1 OE Leads to Increased Organic Acids and Decreased ATP Accumulation

To further understand the increased PSR in *OsHAD1* OE plants at the metabolome level, we performed metabolite profiling of the wild type and OE1. A total of 319 metabolites were detected through gas chromatography-time of flight-mass spectrometry (GC-TOF-MS), of which 90 identified compounds were categorized further into different classes, such as P-containing metabolites, sugars,

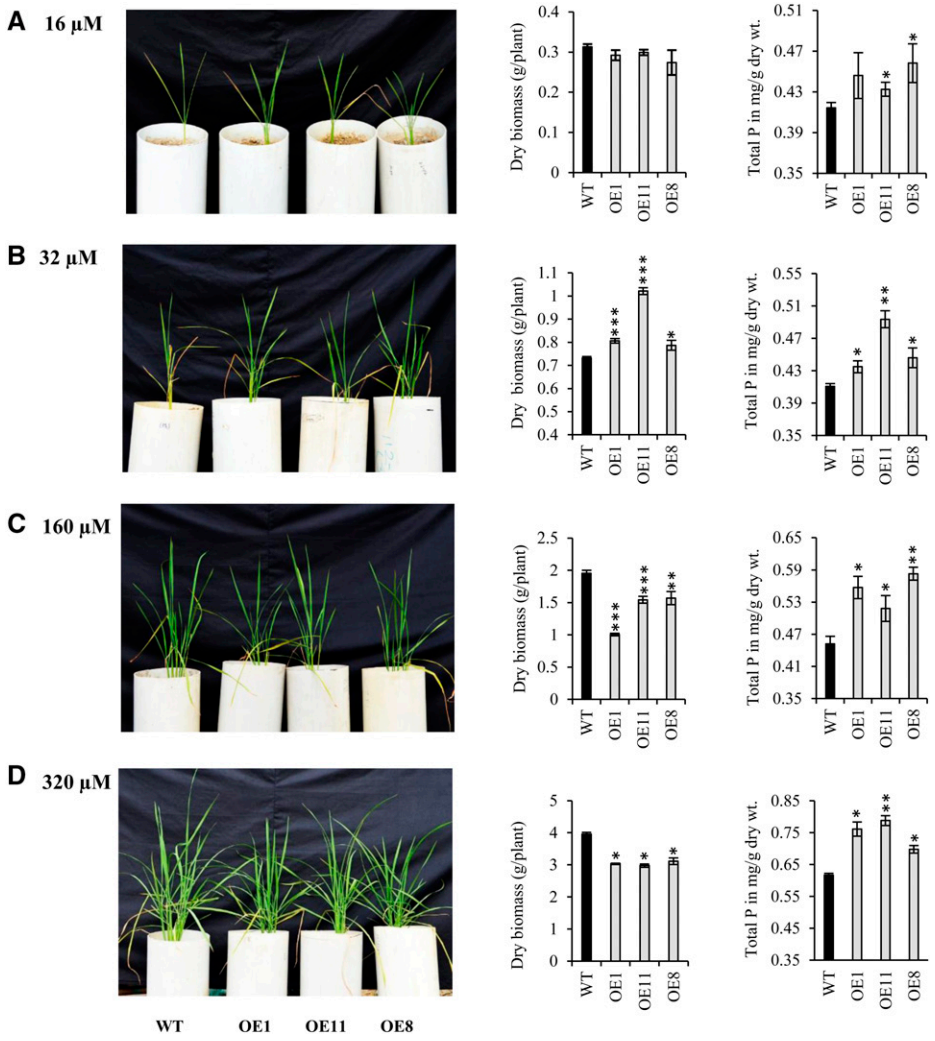

Figure 5. Growth performance and P accumulation in wild-type (WT) and *OsHAD1* overexpressed lines under soil conditions at different Pi concentrations. Plant phenotype, dry biomass, and total P content are shown at 16 μM (A), 32 μM (B), 160 μM (C), and 320 μM (D) Pi. The experiment was set up in three biological replicates. Student's *t* test was used to evaluate significant differences in overexpression lines with respect to the wild type. Asterisks indicate $P \leq 0.05$ (*), $P \leq 0.01$ (**), and $P \leq 0.001$ (***).

acids, amino acids, and others (Supplemental Table S1). Overexpression of *OsHAD1* significantly increased levels of several amino acids and organic acids. Interestingly, most of organic acids, such as oxalic acid, citric acid, malic acid, and succinic acid, were increased significantly in OE1 as compared with the wild type (Fig. 8A; Supplemental Table S1). Elevated levels of these organic acids can help to catalyze faster release of soluble Pi from fixed P sources in the rhizosphere. Furthermore, two of the phosphorylated metabolites, glycerol-α-phosphate and Glc-6-P, were increased significantly in OE1 as compared with the wild type. On the other hand, another P compound, inositol-4-monophosphate, was reduced significantly in OE1 as compared with the wild type (Supplemental Table S1). However, ATP, the most preferred organic substrate of OsHAD1, could not be quantitated in GC-TOF-MS analysis; therefore, we quantitated ATP levels in wild-type and OE lines colorimetrically. Notably, *OsHAD1* OE lines (OE1 and OE11) showed striking depletion of 41% to 48% in ATP levels as compared with the wild type (Fig. 8B). This observation indicates that the increased hydrolysis of intracellular ATP could add to the enhanced P pool in OE lines and subsequent phenotypic alterations. To this end, we conclude that OsHAD1 activates PSR on overexpression in transgenics, which leads to the observed phenotypes.

Identification of OsHAD1-Interacting Proteins

To further understand the molecular regulation by OsHAD1, we performed a pull-down assay to find its interacting partners using *OsHAD1* OE plants. This analysis led to the identification of seven novel putative interactive partners (Table II). One nucleoside diphosphate kinase, OsNDPK3, showed good protein coverage (12%) and high MASCOT scores (131) in liquid chromatography-mass spectrometry analysis. This kinase is known to transfer a Pi group from its His residue to phosphorylate S/T/Y residues in various nucleoside diphosphates. A yeast two-hybrid assay also confirmed the strong interaction of OsHAD1 with OsNDPK3 (Supplemental Fig. S11). Moreover, OsNDPK3 (also

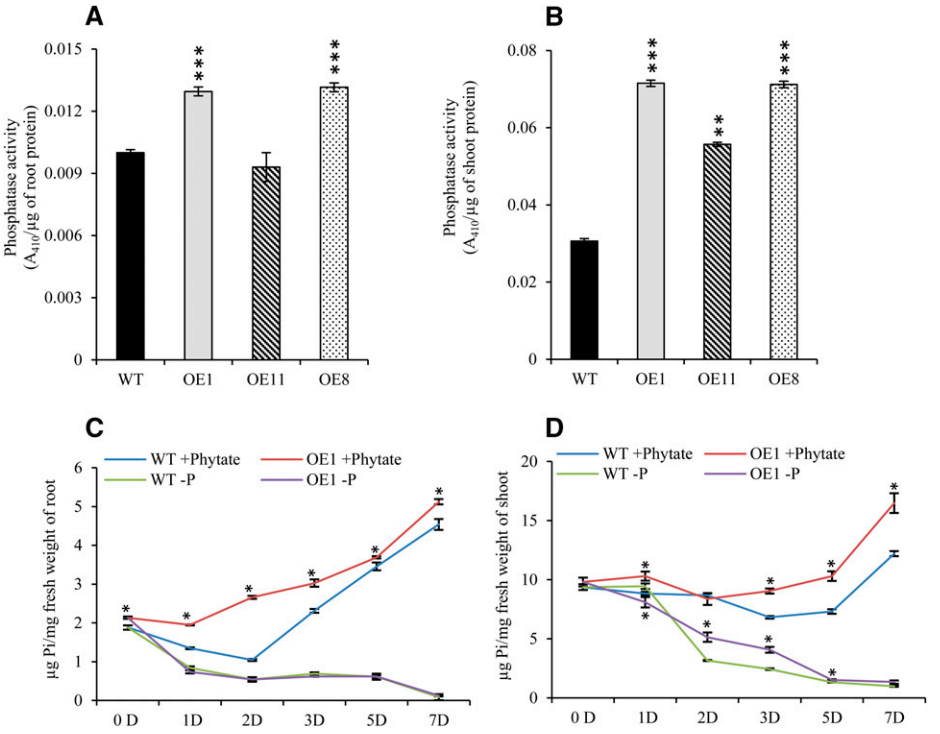

Figure 6. Increased phosphatase activity and soluble P content in *OsHAD1* overexpression lines. A and B, Total acid phosphatase activity in root (A) and shoot (B) of 30-d-old hydroponically raised wild-type (WT) and *OsHAD1* overexpression (OE1, OE11, and OE8) lines raised under +Phytate (100 μM) treatment (15-d-old Pi-deficient plants recovered with 100 μM phytate for another 15 d). Phosphatase activity was quantified with 5 μg of root and 10 μg of shoot protein, respectively, using 10 mM pNPP substrate at 37°C. C and D, Root (C) and shoot (D) soluble P content of the wild type and OE1 at different time points under Pi deficiency and phytate supply. For soluble P estimation, 15-d-old wild-type and *OsHAD1* OE1 plants raised hydroponically under +P conditions were placed in Pi-deficient or phytate-supplied (100 μM) medium. Student's *t* test was used to evaluate significant differences in overexpression lines with respect to the wild type. Asterisks indicate $P \leq 0.05$ (*), $P \leq 0.01$ (**), and $P \leq 0.001$ (***).

found to be low-Pi inducible) was significantly up-regulated in *OsHAD1* OE lines as compared with the wild type (Supplemental Fig. S12). This kinase also was found to coexpress with *OsHAD1* under cytokinin treatment (Supplemental Fig. S13). We also performed interaction studies of OsHAD1 with other rice NDPKs. Interestingly, OsHAD1 also showed strong interaction with OsNDPK1 (Supplemental Fig. S11). The pull-down

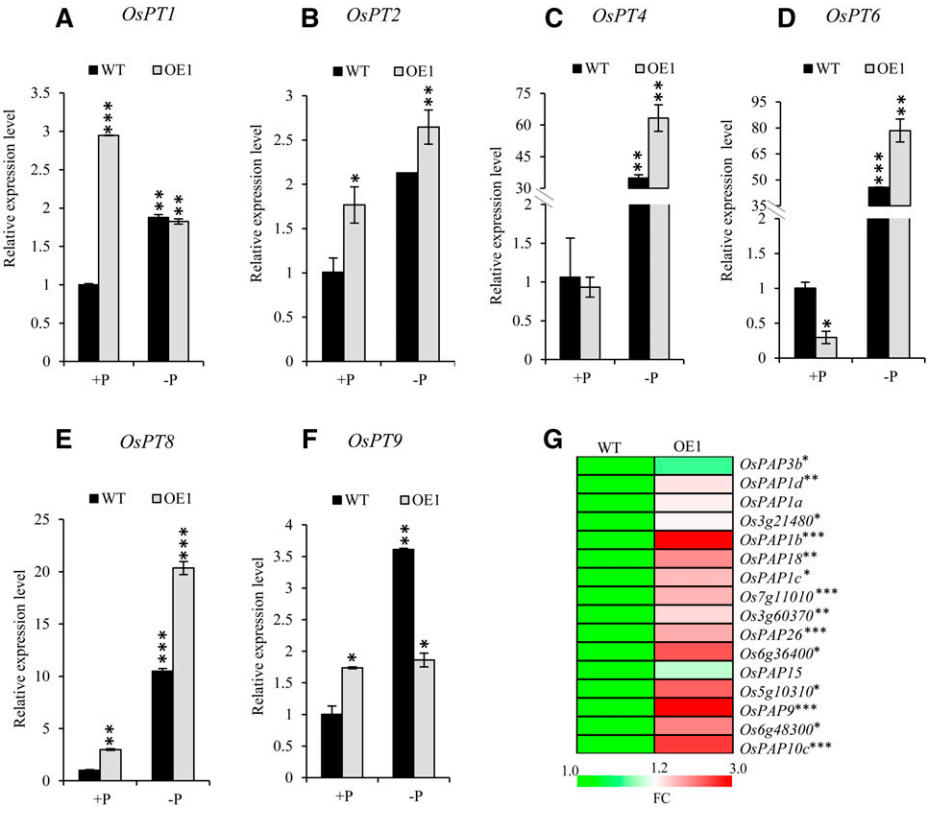

Figure 7. Expression profiling of Pi transporters in wild-type (WT) and *OsHAD1* transgenic plants. A to F, Relative expression levels are shown for *OsPT1* (A), *OsPT2* (B), *OsPT4* (C), *OsPT6* (D), *OsPT8* (E), and *OsPT9* (F) in roots of 30-d-old wild-type and *OsHAD1* overexpression (OE1) plants raised under +P (320 μM) and −P (1 μM) conditions. qRT-PCR was used to determine gene expression, and relative expression level was calculated with respect to the expression level in roots of wild-type +P plants. Each bar represents an average of three replicates with SD. G, Heat map representing relative expression levels (fold change [FC]) of predicted secretory phosphatases/phytases in roots of 30-d-old *OsHAD1* overexpression lines (OE1 and OE11) with respect to the wild type, raised under +P (320 μM). The heat map was generated with MEV 4.6.0. software. Significant changes were determined by Student's *t* test. Asterisks indicate $P \leq 0.05$ (*), $P \leq 0.01$ (**), and $P \leq 0.001$ (***).

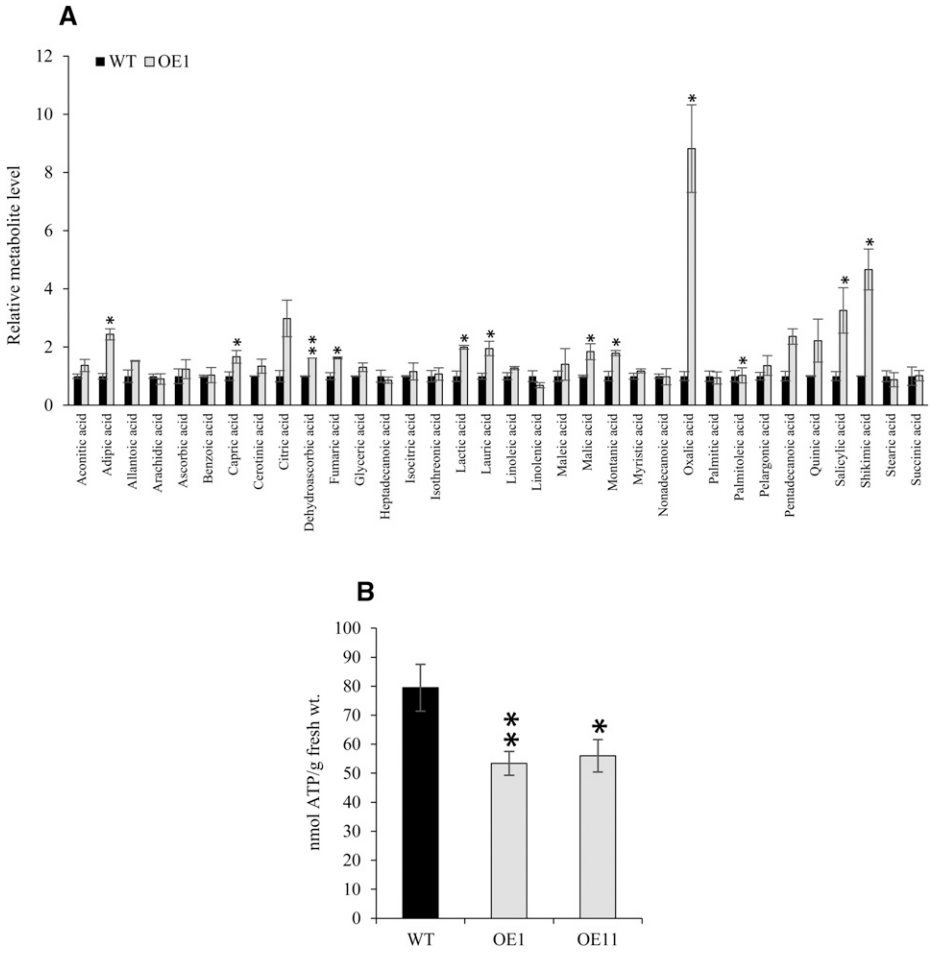

Figure 8. Organic acid accumulation and ATP depletion in *OsHAD1* overexpression lines. A, Relative metabolite levels (ratio of peak heights) in *OsHAD1* OE lines with respect to the wild type (WT). Error bars indicate SE from three biological replicates. B, ATP content in shoots of the wild type and *OsHAD1* overexpression lines (OE1 and OE11). Analyses were carried out in 30-d-old hydroponically raised plants grown under +P conditions (320 μM NaH_2PO_4). Error bars indicate SE from eight replicates. Significant differences in overexpression lines with respect to the wild type were determined by Student's *t* test. Asterisks indicate $P \leq 0.05$ (*) and $P \leq 0.01$ (**).

assay additionally identified one receptor-like kinase (Os10g04730) as an interactive partner of OsHAD1. Notably, it has been shown that the first Asp residue of the DFxDxT/V motif undergoes transient phosphorylation (Baldwin et al., 2001). Thus, these kinases may invariably regulate the OsHAD1 activity by a phosphorylation event. Interestingly, the NetPhos 2.0 prediction server revealed that OsHAD1 possesses 13 Ser, four Tyr, and three Thr residues as phosphorylation sites. Of these, Ser-117, Ser-160, Ser-167, Ser-182, Ser-189, Ser-213, and Tyr-10 are highly predicted (score > 0.93) potential phosphorylation sites. OsHAD1 in close association with these kinases also may regulate the phosphorylation status of downstream targets to activate PSR.

DISCUSSION

Given the indispensable role of P in plant growth and the limited availability of phosphate rocks, enhancing P acquisition and utilization in crops is the key target for sustainable agriculture. Rice is one of most important cereal crops for the developing world. At the same time, rice cultivation requires the highest consumption of Pi fertilizers in countries like India (FAI, 2008; http://www.faidelhi.org/). Therefore, improving the low-P tolerance of rice is a major concern in rice-growing developing nations. Notably, a larger proportion of P exists in the form of organic compounds within cells and the rhizosphere. However, little effort has been devoted to enhancing Pi utilization by releasing bound P from these compounds in rice. Low-Pi-inducible phosphatases play important roles in releasing Pi from bound organic compounds, both intracellularly and extracellularly. The plant HAD superfamily comprises a large number of phosphatases. However, very few low-Pi-inducible phosphatases from the HAD superfamily have been identified and characterized in crop plants (Baldwin et al., 2008; Liang et al., 2012; Zhang et al., 2014). Here, we show that a low-Pi-inducible haloacid dehalogenase, *OsHAD1* encodes a functional acid phosphatase and plays a key role in Pi homeostasis in rice.

This study revealed that *OsHAD1* is a novel low-Pi-responsive APase in rice. Notably, the protein sequence of OsHAD1 does not show significant homology with any other known HAD superfamily phosphatase in plants (Supplemental Fig. S14). However, a multiple sequence alignment showed that OsHAD1 possesses

Table II. *List of putative interacting partners of OsHAD1 identified by liquid chromatography-tandem mass spectrometry analysis combined with electrospray ionization*

Locus Identifier	Score	Putative Function	Nominal Mass	Calculated pI	Protein Coverage
Os05g51700	131	Nucleoside diphosphate kinase	26,124	8.88	12
Os08g34280	41	Cinnamoyl-CoA reductase	47,493	6.34	20
Os02g06770	41	Expressed protein	10,571	9.34	10
Os10g04730	35	TKL_IRAK_DUF26-la.6	47,348	5.38	3
Os02g57140	35	Expressed protein	104,855	5.57	0
Os03g04990	29	Expressed protein	99,020	5.76	1
Os02g10794	19	Expressed protein	207,557	5.32	0

the highly conserved motif I, which is essential for the phosphatase activity of LePS2, OsACP1, PvPS2:2, and GmACP1 phosphatases of the HAD superfamily (Hur et al., 2007; Liang et al., 2012; Zhang et al., 2014). Furthermore, only the four nearest homologs of OsHAD1 in rice shared conserved motifs with OsHAD1 (Supplemental Fig. S15); two of these also showed transcript accumulation under low Pi, although lower than OsHAD1 (Supplemental Fig. S16). This shows that OsHAD1 is unrelated to previously characterized low-Pi-responsive HAD superfamily members. This may be due to the fact that there exists a great degree of sequence divergence among HAD superfamily members (Kuznetsova et al., 2006). This sequence divergence also has been linked to the substrate diversity of HAD proteins (Caparrós-Martín et al., 2013). Although reported members of the HAD superfamily were induced by low Pi, any evidence of their transcriptional regulation was missing. Notably, the expression of many PSR genes is mediated by a MYB transcription factor, OsPHR2, which is a functional ortholog of AtPHR1 in rice (Zhou et al., 2008; Wu et al., 2013; Guo et al., 2015).The physical interaction of OsPHR2 with an *OsHAD1* probe in a gel-shift assay proved that *OsHAD1* acts under OsPHR2-mediated transcriptional regulation.

OsHAD1 possesses both APase and phytase activities and shows a broad substrate specificity. It is important to mention here that most of the PAPs and APases show wide substrate specificity (Kuang et al., 2009; Liang et al., 2010; Tran et al., 2010b; Wang et al., 2011; Cabello-Díaz et al., 2012). It is likely that broad substrate specificity would help to release Pi from various intracellular or extracellular P sources to alleviate Pi starvation. However, to date, no known HAD in rice has been characterized to have broad substrate specificity. Moreover, biochemical properties of OsHAD1, such as high activity in acidic pH and high thermostability, further make it a suitable candidate for improving the low-P tolerance of rice and other crops that are cultivated under higher temperature and acidic ecosystems. Since OsHAD1 is an intracellular and membrane-bound protein, *OsHAD1* also can be overexpressed under a potential signal peptide and targeted in an extracellular milieu for the solubilization of bound P, including phytate. Contradictory to most of the highly low-Pi-responsive PAPs, in silico analysis (using SignalP 4.1, SMART, and PrediSi) of known low-P-responsive HAD superfamily members (such as LePS2, OsACP1, PvPS2:1, PvPS2:2, GmACP1, PvHAD1, AtPECP1, and AtPSPase1) revealed the lack of a potential signal peptide. Additionally, PvPS2:1, PvPS2:2, and LePS2 have been shown to be intracellular protein phosphatases. This indicates that low-Pi-responsive HAD superfamily proteins are destined to play some unknown cellular signaling roles under Pi deficiency.

OsHAD1 OE lines showed higher P accumulation than the wild type under +P, −P, and restricted P supply (+Phytate) in hydroponics, soil conditions, as well as in aseptic agar (Figs. 4–6; Supplemental Figs. S6 and S17). This indicates high Pi acquisition in OE lines irrespective of the degree/type of P supply. However, under high-Pi conditions, OE lines showed retarded growth as compared with the wild type, which could be due to enhanced P accumulation. Previous studies also have reported growth retardation due to high Pi accumulation in rice. For instance, it is known that *OsPHR2* overexpression resulted in excessive P accumulation in rice shoots, leading to retarded growth under sufficient Pi (Zhou et al., 2008). Higher Pi accumulation in OsPHR2 OE lines was attributed to increased expression of several PSR genes, such as *OsPT*s (Zhou et al., 2008). Likewise, overexpression/suppression of many PSR genes, like *OsMyb2P-1*, *OsSPX1*, *OsmiR399*, and *ltn1*, showed overaccumulation of P and retarded growth under sufficient Pi (Wang et al., 2009; Hu et al., 2011; Dai et al., 2012). Overexpression of OsHAD1 activated the phosphate starvation response in rice seedlings. Elevated expression of secretory phytases/phosphatases and PSR phosphate transporters in OsHAD1 OE lines further strengthens the signaling role for OsHAD1 in Pi homeostasis. Several studies have shown that increased expression of PSR transporters and phosphatases/phytases is involved directly in the higher P accumulation (Zhou et al., 2008; Tran et al., 2010a; Kong et al., 2014). Furthermore, overexpression of *OsPT8* (also up-regulated in *OsHAD1* OE1) showed excessive P accumulation under high-P conditions (Jia et al., 2011). OsPT8 is membrane localized, and OsHAD1 also showed signal in membrane. Coexpression and qRT-PCR analysis of *OsHAD1* showed that both *OsHAD1* and *OsPT8* are down-regulated in shoot when treated with cytokinin (Supplemental

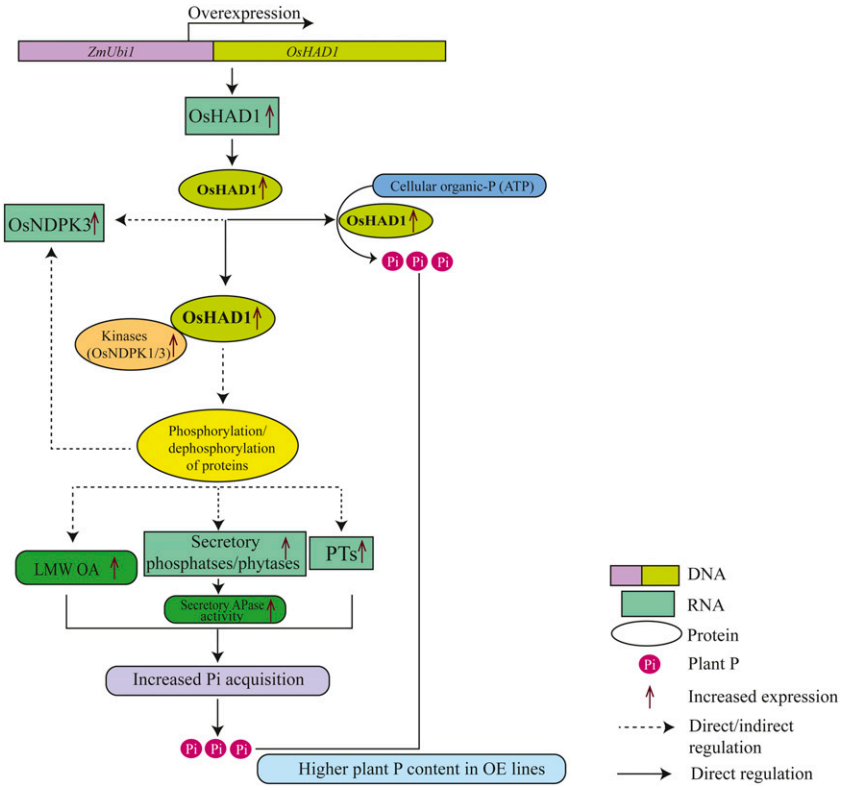

Figure 9. Model for enhanced P accumulation in *OsHAD1* overexpression lines. Constitutive expression of *OsHAD1* under the control of the maize (*Zea mays*) ubiquitin promoter (*ZmUbi1*) in rice leads to increased P content by direct or indirect routes. Increased expression of OsHAD1 (protein phosphatase) along with interacting kinases affects the phosphorylation status of unknown downstream targets, which increases the expression of PSR Pi transporters (PTs), phosphatases/phytases, and the accumulation of low-molecular-weight organic acids (LMW OA). Overexpression of OsHAD1 also leads to increased expression of its interacting kinase, OsNDPK3. Increased phosphatase activity of OsHAD1 remobilizes P from cellular ATP. These events ultimately lead to increased Pi acquisition in *OsHAD1* overexpression lines.

Fig. S13), a known suppressor of PSR genes under low-P conditions (Martín et al., 2000; Hou et al., 2005; Lai et al., 2007).

Notably, like overexpression of intracellular HAD, *PvPS2:1* also was found to up-regulate the transcripts of a PSR Pi transporter, leading to enhanced P content and superior P efficiency in Arabidopsis OE lines as compared with the wild type (Liang et al., 2012). Apart from these findings, well-known low-Pi responses such as increased secretory APase activity, accumulation of organic acids (Pant et al., 2015), and decreased levels of ATP (Mikulska et al., 1998) in OE lines indicate that *OsHAD1* is involved in regulating PSR. Reduction in ATP content also could be caused by increased phosphatase activity of OsHAD1, as ATP was found to be the most preferred substrate of OsHAD1. Increased ATP hydrolysis by ATP can add to the cellular Pi pool and enhance internal Pi utilization efficiency.

Reversible phosphorylation, mediated by PSR phosphatases and kinases, is one of the prominent post-translational modifications that regulate Pi homeostasis (Lan et al., 2013; Li et al., 2014). Regulation of the phosphorylation status of proteins can affect their activity, stability, structure, localization, and interactions (Lan et al., 2013). Some of the proteins, such as AtPHT1;1 and Pho4, are reported to be regulated by reversible phosphorylation under Pi deficiency in Arabidopsis and yeast, respectively (Springer et al., 2003; Bayle et al., 2011). Several kinases and phosphatases are differentially regulated by Pi deficiency (Wu et al., 2003; Fragoso et al., 2009; Gamuyao et al., 2012; Lan et al., 2012). Some of these also are suggested to play pivotal roles in maintaining Pi homeostasis through modifying the phosphorylation status of downstream targets. For instance, overexpression of a protein kinase-encoding PSR gene, *OsPSTOL1*, was hypothesized to regulate the phosphorylation of unknown targets, leading to the induction of numerous genes involved in root proliferation and, thus, Pi uptake (Gamuyao et al., 2012). Unlike protein kinases, protein phosphatases form a small group of proteins but can associate themselves with a huge number of target proteins and regulate their functions (Wang et al., 2007; Plaxton and Shane, 2015). Overexpression of a Ser/Thr phosphatase-encoding HAD gene, *LePS2*, resulted in delayed plant development and increased APase activity and anthocyanin content in transgenic tomato (Baldwin et al., 2008). The altered phosphorylation of unknown targets by LePS2 was proposed to initiate an unknown signaling cascade that led to distinct changes in plant morphology. OsHAD1 showed protein phosphatase activity, cytoplasmic location, and regulation by OsPHR2; therefore, it might play key signaling roles leading to the enhanced PSR observed in our study.

Overexpression of OsHAD1 in rice also might have influenced the phosphorylation status of several target proteins, leading to the induction of Pi transporters, phytases, protein phosphatases, and genes involved in organic acid production. Interestingly, phosphatases of the HAD superfamily have been reported to share

similar active site geometries, folds, and reaction chemistry to the response regulator signaling protein of a two-component signaling system (His kinase phosphatase) in bacteria (Ridder and Dijkstra, 1999; Immormino et al., 2015). Moreover, OsHAD1 showed an association with kinases. Of these, NDPKs play important roles in several signal transduction pathways and play important roles in various abiotic and biotic stresses (for review, see Dorion and Rivoal, 2015). Thus, OsHAD1 in coordination with protein kinases may regulate the phosphorylation status of downstream targets to regulate Pi homeostasis in plants (Fig. 9). The effect of this signaling is apparent in the form of the induction of several genes and alterations in metabolite profile that ultimately led to increased plant P content (Fig. 9).

Taken together, our work provides a novel resource to improve the Pi utilization ability of rice. Since only ~20% of applied P is assimilated by crops in a year and the rest becomes fixed in soil, sustainable agriculture using crops with improved Pi use efficiency would be helpful in reducing the use of Pi fertilizers and their escape in the environment.

MATERIALS AND METHODS

Plant Materials and Growth Conditions

Seeds of the rice (*Oryza sativa*) genotypes Dular and PB1 were surface sterilized and germinated as described earlier (Mehra et al., 2016). Uniformly germinated seeds were transferred to Pi-sufficient (320 μM) and Pi-deficient (1 μM) Yoshida media as described (Mehra et al., 2015). Seedlings were raised in growth chambers at 30°C (16 h)/28°C (8 h), ~70% relative humidity, and 280 to 300 μmol photons m^{-2} s^{-1}. For *OsHAD1* expression analysis, root and shoot from +P and –P seedlings were profiled after 5, 15, and 21 d of treatment. For expression analysis under different nutrient deficiency conditions (−N, −P, −K, −Fe, and −Zn), seedlings were raised hydroponically as described (Singh et al., 2015). Root tissues were collected after 7 and 15 d of the respective deficiency treatments.

To analyze the effect of cytokinin on gene expression, 15-d-old hydroponically raised seedlings were given cytokinin (2 μM BAP) treatment for variable times (0.5, 1, and 2 h). Seedlings were harvested and frozen in liquid nitrogen after the respective time points.

For the analysis of *OsHAD1* OE lines in hydroponics, the wild type and three independent T3 homozygous transgenic lines were grown hydroponically under +P and –P for 15 d as explained above. Thereafter, half of the –P seedlings were supplied with 100 μM phytate as a restricted P source for an additional 15 d. Thirty-day-old wild-type and transgenic plants were harvested for downstream phenotypic, biochemical, and molecular analyses.

For soil-based experiments, seedlings were raised in hydroponics under +P and –P for 20 d. Afterward, seedlings were transferred to one-end-closed PVC pipes (42 cm × 9.5 cm) filled with washed sand:soilrite:vermiculite (2:1:1). One seedling per pipe was maintained. Eight replicates of both the wild type and three overexpression lines were arranged randomly in 4 × 8 arrays. The whole experiment was performed with three such arrays. The first array was planted with seedlings raised in +P medium, while the other two arrays were planted with –P seedlings. All three arrays were fed with 1 L of the respective +P and –P Yoshida solutions per day per pipe. After 5 d, one array of −P-raised seedlings was recovered with 100 μM phytate-supplemented Yoshida medium for the next 25 d. The other two arrays were continually supplied with their respective +P and –P Yoshida solutions for 25 d. Thus, 50-d-old plants from all three arrays were harvested for phenotypic analysis and total P content. This experiment was carried out in a greenhouse maintained at 30°C (16 h)/28°C (8 h) and ~70% relative humidity.

For P content analysis under the aseptic condition, germinated seeds were placed in one-half-strength Murashige and Skoog medium containing 100 μM phytate for 7 d. For soluble Pi content analysis, 15-d-old hydroponically raised +P plants of the wild type and OE1 were subjected to Pi-deficient medium and 100 μM phytate-supplemented medium separately. Root and shoot tissues were frozen at different time points (0, 1, 2, 3, 5, and 7 d) of Pi deficiency and phytate treatment, respectively.

RNA extraction and qRT-PCR were performed as described (Mehra and Giri, 2016) using gene-specific primers (Supplemental Table S2). Total and soluble P estimation was performed as described (Mehra et al., 2016, 2017). The statistical significance of relative expression levels (fold changes) was evaluated using Student's *t* test.

Gel Retardation Assay

The coding region of *OsPHR2* was amplified using gene-specific forward and reverse primers (Supplemental Table S2) carrying *Nde*I and *Bam*HI restriction sites, respectively, and cloned in pET28a expression vector (Novagen). 6xHis-tagged OsPHR2 was purified using Ni^{2+} affinity chromatography as described (Mehra and Giri, 2016). The 485-bp promoter region of *OsHAD1* was amplified using gene-specific primers (Supplemental Table S2) and used as a probe. The promoter probe was labeled with [α-^{32}P]CTP using the Megaprime DNA labeling system kit (Amersham Biosciences) according to the manufacturer's protocol. Three different reactions were set: the first reaction contained 12.74 ng of [α-^{32}P]CTP-labeled *OsHAD1* promoter probe only; the second reaction contained 1.5 μg of OsPHR2 protein with 12.74 ng of labeled probe; and the third reaction contained 1.5 μg of OsPHR2 protein, 12.74 ng of labeled probe, with a 100× concentration of unlabeled probe (competitor). All three reactions were incubated with 1 μg of poly(dI-dC), 30 mM KCl, 15 mM HEPES (pH 8), 0.02 mM DTT, 1 mM $MgCl_2$, 0.2 mM EDTA, and 0.6% glycerol at 37°C for 30 min. Thereafter, all reactions were electrophoresed on a 4% polyacrylamide gel for 8 h at 100 V. The gel was exposed to a phosphor screen overnight. The image was captured with the Typhoon 9210 phosphor imager (GE Healthcare).

Expression, Purification, and APase Assays of Recombinant OsHAD1 (Wild Type and Mutated)

The coding region of *OsHAD1* was amplified with gene-specific terminal primers (OsHAD1_pET28a F and OsHAD1_pET28a R; Supplemental Table S2). For site-directed mutagenesis, the D16A and D18A mutant versions of OsHAD1 were generated by an overlap extension PCR method as described (Ho et al., 1989). Mutated PCR amplicons were generated using terminal primers (OsHAD1_pET28a) and overlapping primers (OsHAD1_SDM_overlap) with desired mutations (Supplemental Table S2). Wild-type and mutagenized OsHAD1 coding sequences were cloned into *Bam*HI and *Eco*RI sites of the 6xHis expression vector pET28a. Recombinant wild-type/mutagenized OsHAD1 protein was induced in *Escherichia coli* strain BL21(DE3)pLysS with 100 mM isopropylthio-β-galactoside and purified by Ni^{2+} affinity chromatography (Mehra and Giri, 2016). Five micrograms of purified D16A, D18A, and wild-type OsHAD1 proteins was used for the APase assay in a 100-μL reaction containing 10 mM pNPP as substrate, 5 mM $MgCl_2$, and 50 mM sodium acetate (pH 6). Reactions were incubated at 37°C for 30 min. The amount of Pi released was quantified by adding 100 μL of ammonium molybdate reagent (Kitson and Mellon, 1944). Released Pi was estimated by measuring A_{410} using POLARstar Omega (BMG Labtech) in at least three replicates.

Biochemical Characterization of OsHAD1

pH and Temperature Optima of OsHAD1

The pH optimum of OsHAD1 was determined at various pH levels (2, 5, 6, 7, 7.4, 8, and 8.8) in a reaction containing 10 mM substrate (pNPP, ATP, AMP, and Rib-5-P), 5 mM $MgCl_2$, and 10 μg of recombinant OsHAD1 protein at 37°C for 30 min. A 50 mM concentration of sodium acetate and Tris-Cl buffer were used to set the pH range from pH 2 to 6 and pH 7 to 8.8, respectively. To determine the optimum temperature of OsHAD1, activity assays of OsHAD1 were performed for 30 min at different temperatures (25°C–75°C) in a reaction containing 10 μg of purified OsHAD1 protein, 5 mM $MgCl_2$, 50 mM sodium acetate buffer (pH 6), and 10 mM pNPP. Released Pi was measured by the yellow vanadomolybdate method.

Substrate Specificity and OsHAD1 Reaction Kinetics

To determine the substrate specificity of OsHAD1, various P-containing compounds (pNPP, ATP, ADP, AMP, inorganic pyrophosphate, sodium phytate, *O*-phosphoserine, *O*-phosphothreonine, Glc-6-P, Fru-6-P, Man-6-P, Rib-5-P, dRib-5-P, and α-D-Man-1-P) were used. Activity assays were performed with 10 mM of different substrates as described above. For the kinetics study, activity assays were carried out with ATP and pNPP as substrates over a wide range of concentrations (0.1, 0.15, 0.2, 0.25, 0.5, 1, 1.25, 2, 5, 10, 15, 20, 25, 50, 75, and 100 mM). Specific activity and K_m were calculated from a Lineweaver-Burk plot. All reactions were performed in triplicate.

Effects of Different Ions and Inhibitors on the Phosphatase Activity of OsHAD1

The phosphatase activity of OsHAD1 was analyzed with 10 mM chloride salts of different cations (Mn^{2+}, Na^+, K^+, Ca^{2+}, Co^{2+}, Mg^{2+}, Cu^{2+}, and Ni^{2+}) and 10 mM sodium salts of different anions (EDTA, citrate, molybdate, phosphate, thiosulfate, bicarbonate, and sulfate). Reactions were performed in three replicates with 10 mM pNPP as described above.

Exogenous Application of OsHAD1 to Wild-Type Seedlings

Rice seedlings were raised hydroponically in five separate containers in three biological replicates. One container was supplied with 320 μM NaH_2PO_4 (+P) while four others were supplied with 1 μM NaH_2PO_4 (−P) for 15 d. Each container contained 20 seedlings. After 15 d, Pi-starved seedlings in three of the containers were recovered with 100 μM phytate (Sigma; P8810) as the P source. Out of these three containers, two were supplemented with 125 ng mL^{-1} purified recombinant OsHAD1 wild-type or mutated protein (D16A). Seedlings were recovered for another 7 d. The rest of the seedlings in +P and –P medium-containing containers continued to be raised in their respective nutrient media for another 7 d. After this, the seedlings were harvested for phenotypic and total P content analyses.

Vector Construction and Development of Transgenic Lines

Full-length cDNA (AK240756) of *OsHAD1* was amplified using gene-specific primers (Supplemental Table S2) and cloned under the control of the *ZmUbi1* promoter in a Gateway-compatible overexpression vector, pANIC6B (Mann et al., 2012). The overexpression construct was transformed into *Agrobacterium tumefaciens* strain EHA105 and introduced into rice calli by the *A. tumefaciens*-mediated transformation method as described (Toki et al., 2006). Regenerated plants were selected on hygromycin (50 μg mL^{-1}) and screened by PCR with *hptII* gene-specific primers and GUS histochemical staining.

Phosphatase and Phytase Activity Assay in Wild-Type and Transgenic Plants

Total protein was extracted from 250 mg of frozen roots and shoots of 30-d-old hydroponically raised (+Phytate) wild-type and *OsHAD1* transgenic plants in chilled extraction buffer (100 mM potassium acetate, 20 mM $CaCl_2$, 2 mM EDTA, 0.1 mM phenylmethylsulfonyl fluoride, and 20% glycerol, pH 6) as described (Mehra et al., 2017). For total phosphatase activity, 20 μg of extracted protein was incubated with 10 mM pNPP, 5 mM $MgCl_2$, and 50 mM sodium acetate buffer (pH 6) in a total volume of 100 μL. Reactions were performed at 37°C for 15 min. Released Pi was measured by the yellow vanadomolybdate method (Kitson and Mellon, 1944). For phytase activity, reactions were performed with 40 μg of total protein and 10 mM sodium phytate as substrate.

For the estimation of secretory APase activity, wild-type and OE1 seedlings were raised hydroponically under +P and –P conditions for 12 d. After this, 10 plants each of the wild type or OE1 were kept in 100 mL of +P or –P medium in a glass tube. After 3 d, liquid medium was collected from each tube and filtered. The secretory APase activity assay was performed as described previously (Mehra et al., 2017). A total of 800 μL of filtered medium was incubated with 5 mM pNPP at 37°C for 1 h. Reactions were stopped by 100 μL of 0.4 M NaOH. APase activity was quantitated spectrophotometrically at 410 nm. The whole experiment was performed in three replicates.

Subcellular Localization of the OsHAD1:YFP Fusion Protein

The coding sequence of *OsHAD1* was fused in frame with the coding sequence of YFP by cloning in pSITE-3CA using the Gateway cloning system (Invitrogen). Particle bombardment assays were performed on onion (*Allium cepa*) epidermal cells as described earlier (Mehra et al., 2017). For transient expression in *Nicotiana benthamiana*, the *OsHAD1* construct in pSITE-3CA was transformed into *A. tumefaciens* strain GV3101. Agroinfiltration of *N. benthamiana* was carried out according to Walter et al. (2004). For plasmolysis, epidermal cells were exposed to 5% NaCl solution for a few seconds. Images were analyzed using the AOBS TCS-SP2 (Leica) confocal microscope.

Metabolite Profiling and ATP Estimation

For metabolite profiling and ATP estimation, 30-d-old +P-grown wild-type and OsHAD1 OE lines were used. For metabolite extraction, 1 mg of lyophilized leaves was ground in 1 mL of prechilled solvent (methanol:chloroform:water, 5:2:2, v/v/v) for 30 s at 1,500 rpm using a Retsch ball mill. Samples were vortexed for 6 min at 4°C followed by centrifugation at 14,000 rcf for 2 min. Clear supernatant was collected and dried in a Labconco Centrivap cold trap concentrator. Extracts were derivatized and prepared for GC-TOF-MS using the ALEX-CIS GC-TOF-MS apparatus as described (Fiehn et al., 2008). The experiment was performed in three replicates.

ATP estimation was performed according to Zeng et al. (2013). Briefly, 100 mg of leaf samples of 30-d-old +P-grown wild-type and OsHAD1 OE1 plants was crushed in liquid nitrogen. Ground samples were mixed immediately with 400 μL of 0.0005% (v/v) perchloric acid and boiled for 10 min in a water bath. The whole mixture was centrifuged at 13,000 rpm for 15 min at 4°C, and a clear supernatant was collected for ATP estimation using an ATP colorimetric assay kit (Sigma; MAK190). Quantitation was done from eight independent replicates.

Immunoblotting of OsHAD1

A total of 40 μg of protein extract was electrophoresed on 12% SDS-PAGE. Subsequently, proteins were transferred to a polyvinylidene difluoride membrane (Millipore) in a western-blot tank according to the manufacturer's protocol. The membrane was blocked with 5% (w/v) skim milk in PBST buffer overnight. Immunodetection of OsHAD1 was carried out by incubating with primary antibody (anti-OsHAD1 raised in rabbit) in 5% skim milk for 2 h followed by three gentle washings with PBST buffer for 5, 10, and 5 min. After washing, the membrane was incubated with secondary antibody diluted in 5% skim milk for 2 h. Following two washings, each for 10 min, OsHAD1 protein was detected by incubating the membrane in BCIP-NBT (Sigma; B1911) substrate for 2 min.

Pull-Down and Yeast Two-Hybrid Assays

The coding region of *OsHAD1* was fused with GST tag by cloning in pGEX4T-1 expression vector (Amersham Biosciences). Recombinant OsHAD1 and empty pGEX4T-1 vector were independently transformed and induced in *E. coli* strain BL21(DE3)pLysS as described above. Recombinant OsHAD1 was immobilized on GST beads (Sigma; G4510) according to the manufacturer's protocol. Interactome analysis through GST pull down was performed as described (Datta et al., 2015). Briefly, total protein from 30-d-old +P-grown *OsHAD1* OE1 was extracted using extraction buffer (1 mM DTT, 1 mM phenylmethylsulfonyl fluoride, 1 mM EDTA [pH 8], in 1× phosphate-buffered saline, pH 7.4). Total plant protein was incubated with OsHAD1-GST-bound agarose beads at 4°C overnight. Furthermore, the beads were washed with 1× phosphate-buffered saline three times for 10 min with gravity flow. Proteins bound with GST beads were eluted with 20 mM glutathione at pH 8. Eluted proteins were electrophoresed on 12% SDS-PAGE. Separated protein bands were identified with liquid chromatography-mass spectrometry combined with electrospray ionization as described earlier (Jaiswal et al., 2013).

Yeast two-hybrid assays were performed using the Matchmaker Gold Yeast two-hybrid system (Clontech) according to the manufacturer's protocol. The coding sequence of OsHAD1 was cloned into the bait vector pGBKT7 (BD). The coding sequences of OsNDPK1, OsNDPK2, and OsNDPK3 were cloned into the prey vector pGADT7 (AD). AD and BD clones were cotransformed in yeast strain Y2H Gold (Clontech) and selected on minimal medium, His, Leu, and Trp, and adenine, His, Leu, and Trp.

Supplemental Data

The following supplemental materials are available.

Supplemental Figure S1. Expression profiling of *OsHAD1* in different tissues and developmental stages.

Supplemental Figure S2. Induction and purification of OsHAD1 recombinant protein.

Supplemental Figure S3. Asp residues of motif I are essential for the activity of OsHAD1.

Supplemental Figure S4. Confirmation of *OsHAD1* overexpression lines for transgenic nature.

Supplemental Figure S5. Phenotype of *OsHAD1* overexpressed lines grown in soil under +P, −P, and phytate recovery conditions.

Supplemental Figure S6. Effects of *OsHAD1* overexpression on biomass and total P content of plants grown in soil.

Supplemental Figure S7. Transient expression of YFP-OsHAD1 in onion epidermal cells.

Supplemental Figure S8. Transient expression of YFP-OsHAD1 in *N. benthamiana*.

Supplemental Figure S9. Phytase activity of the wild type and *OsHAD1* overexpression lines raised under phytate recovery.

Supplemental Figure S10. Overexpression of *OsHAD1* increased secretory APase activity in rice.

Supplemental Figure S11. Yeast two-hybrid assay of OsHAD1 with OsNDPK1/2/3.

Supplemental Figure S12. Expression profile of *OsNDPK3*.

Supplemental Figure S13. Coexpression of *OsHAD1* with *OsPT8* and *OsNDPK3* under cytokinin treatment.

Supplemental Figure S14. Sequence alignment of OsHAD1 with known low-P-responsive HAD superfamily members.

Supplemental Figure S15. Amino acid sequence alignment of OsHAD1 with its nearest rice homologs.

Supplemental Figure S16. Expression profile of *OsHAD1* and its nearest homologs in rice under the P-deficient condition in Dular and PB1 roots and shoots.

Supplemental Figure S17. P profile and dry biomass of the wild type and *OsHAD1* overexpression lines grown under low-P or phytate supply.

Supplemental Table S1. List of metabolites identified in *OsHAD1* OE lines and the wild type using ALEX-CIS GC-TOF-MS.

Supplemental Table S2. List of primers used in this study.

ACKNOWLEDGMENTS

We acknowledge the phytotron facility at the National Institute of Plant Genome Research. B.K.P. and J.B. acknowledge research fellowships from DBT. P.M and L.V. acknowledge research fellowships from CSIR.

Received April 26, 2017; accepted June 17, 2017; published June 21, 2017.

LITERATURE CITED

Baldwin JC, Karthikeyan AS, Cao A, Raghothama KG (2008) Biochemical and molecular analysis of LePS2;1: a phosphate starvation induced protein phosphatase gene from tomato. Planta **228:** 273–280

Baldwin JC, Karthikeyan AS, Raghothama KG (2001) *LEPS2*, a phosphorus starvation-induced novel acid phosphatase from tomato. Plant Physiol **125:** 728–737

Bayle V, Arrighi JF, Creff A, Nespoulous C, Vialaret J, Rossignol M, Gonzalez E, Paz-Ares J, Nussaume L (2011) *Arabidopsis thaliana* high-affinity phosphate transporters exhibit multiple levels of posttranslational regulation. Plant Cell **23:** 1523–1535

Burroughs AM, Allen KN, Dunaway-Mariano D, Aravind L (2006) Evolutionary genomics of the HAD superfamily: understanding the structural adaptations and catalytic diversity in a superfamily of phosphoesterases and allied enzymes. J Mol Biol **361:** 1003–1034

Cabello-Díaz JM, Quiles FA, Lambert R, Pineda M, Piedras P (2012) Identification of a novel phosphatase with high affinity for nucleotides monophosphate from common bean (*Phaseolus vulgaris*). Plant Physiol Biochem **53:** 54–60

Caparrós-Martín JA, McCarthy-Suárez I, Culiáñez-Macià FA (2013) HAD hydrolase function unveiled by substrate screening: enzymatic characterization of *Arabidopsis thaliana* subclass I phosphosugar phosphatase AtSgpp. Planta **237:** 943–954

Chien SH, Prochnow LI, Tu S, Snyder CS (2011) Agronomic and environmental aspects of phosphate fertilizers varying in source and solubility: an update review. Nutr Cycl Agroecosyst **89:** 229–255

Cordell D, Neset TS (2014) Phosphorus vulnerability: a qualitative framework for assessing the vulnerability of national and regional food systems to the multi-dimensional stressors of phosphorus scarcity. Glob Environ Change **24:** 108–122

Dai X, Wang Y, Yang A, Zhang WH (2012) OsMYB2P-1, an R2R3 MYB transcription factor, is involved in the regulation of phosphate-starvation responses and root architecture in rice. Plant Physiol **159:** 169–183

Datta A, Kamthan A, Kamthan M (2015) A simple protocol to detect interacting proteins by GST pull down assay coupled with MALDI or LC-MS/MS analysis. Protocol Exchange doi/10.1038/protex.2015.093

Dobermann A, Cassman KG, Mamaril CP, Sheehy JE (1998) Management of phosphorus, potassium, and sulfur in intensive, irrigated lowland rice. Field Crops Res **56:** 113–138

Dorion S, Rivoal J (2015) Clues to the functions of plant NDPK isoforms. Naunyn Schmiedebergs Arch Pharmacol **388:** 119–132

Fiehn O, Wohlgemuth G, Scholz M, Kind T, Lee DY, Lu Y, Moon S, Nikolau B (2008) Quality control for plant metabolomics: reporting MSI-compliant studies. Plant J **53:** 691–704

Fragoso S, Espíndola L, Páez-Valencia J, Gamboa A, Camacho Y, Martínez-Barajas E, Coello P (2009) SnRK1 isoforms AKIN10 and AKIN11 are differentially regulated in Arabidopsis plants under phosphate starvation. Plant Physiol **149:** 1906–1916

Gamuyao R, Chin JH, Pariasca-Tanaka J, Pesaresi P, Catausan S, Dalid C, Slamet-Loedin I, Tecson-Mendoza EM, Wissuwa M, Heuer S (2012) The protein kinase Pstol1 from traditional rice confers tolerance of phosphorus deficiency. Nature **488:** 535–539

George TS, Simpson RJ, Gregory PJ, Richardson AE (2007) Differential interaction of *Aspergillus niger* and *Peniophora lycii* phytases with soil particles affects the hydrolysis of inositol phosphates. Soil Biol Biochem **39:** 793–803

Guo M, Ruan W, Li C, Huang F, Zeng M, Liu Y, Yu Y, Ding X, Wu Y, Wu Z, et al (2015) Integrative comparison of the role of the PHOSPHATE RESPONSE1 subfamily in phosphate signaling and homeostasis in rice. Plant Physiol **168:** 1762–1776

Ha S, Tran LS (2014) Understanding plant responses to phosphorus starvation for improvement of plant tolerance to phosphorus deficiency by biotechnological approaches. Crit Rev Biotechnol **34:** 16–30

Harrison AF (1987) Soil Organic Phosphorus: A Review of World Literature. CAB International, Wallingford, UK

Ho SN, Hunt HD, Horton RM, Pullen JK, Pease LR (1989) Site-directed mutagenesis by overlap extension using the polymerase chain reaction. Gene **77:** 51–59

Hou XL, Wu P, Jiao FC, Jia QJ, Chen HM, Yu J, Song XW, Yi KK (2005) Regulation of the expression of OsIPS1 and OsIPS2 in rice via systemic and local Pi signalling and hormones. Plant Cell Environ **28:** 353–364

Hu B, Zhu C, Li F, Tang J, Wang Y, Lin A, Liu L, Che R, Chu C (2011) LEAF TIP NECROSIS1 plays a pivotal role in the regulation of multiple phosphate starvation responses in rice. Plant Physiol **156:** 1101–1115

Hur YJ, Lee HG, Jeon EJ, Lee YY, Nam MH, Yi G, Eun MY, Nam J, Lee JH, Kim DH (2007) A phosphate starvation-induced acid phosphatase from *Oryza sativa*: phosphate regulation and transgenic expression. Biotechnol Lett **29:** 829–835

Immormino RM, Starbird CA, Silversmith RE, Bourret RB (2015) Probing mechanistic similarities between response regulator signaling proteins and haloacid dehalogenase phosphatases. Biochemistry **54:** 3514–3527

Jaiswal DK, Ray D, Choudhary MK, Subba P, Kumar A, Verma J, Kumar R, Datta A, Chakraborty S, Chakraborty N (2013) Comparative

proteomics of dehydration response in the rice nucleus: new insights into the molecular basis of genotype-specific adaptation. Proteomics **13:** 3478–3497

Jia H, Ren H, Gu M, Zhao J, Sun S, Zhang X, Chen J, Wu P, Xu G (2011) The phosphate transporter gene OsPht1;8 is involved in phosphate homeostasis in rice. Plant Physiol **156:** 1164–1175

Kirk GJD, George T, Courtois B, Senadhira D (1998) Opportunities to improve phosphorus efficiency and soil fertility in rainfed lowland and upland rice ecosystems. Field Crops Res **56:** 73–92

Kitson RE, Mellon MG (1944) Colorimetric determination of phosphorus as molybdivanadophosphoric acid. Ind Eng Chem Anal Ed **16:** 379–383

Kong Y, Li X, Ma J, Li W, Yan G, Zhang C (2014) *GmPAP4*, a novel purple acid phosphatase gene isolated from soybean (*Glycine max*), enhanced extracellular phytate utilization in *Arabidopsis thaliana*. Plant Cell Rep **33:** 655–667

Kuang R, Chan KH, Yeung E, Lim BL (2009) Molecular and biochemical characterization of AtPAP15, a purple acid phosphatase with phytase activity, in Arabidopsis. Plant Physiol **151:** 199–209

Kuznetsova E, Proudfoot M, Gonzalez CF, Brown G, Omelchenko MV, Borozan I, Carmel L, Wolf YI, Mori H, Savchenko AV, et al (2006) Genome-wide analysis of substrate specificities of the *Escherichia coli* haloacid dehalogenase-like phosphatase family. J Biol Chem **281:** 36149–36161

Lai F, Thacker J, Li Y, Doerner P (2007) Cell division activity determines the magnitude of phosphate starvation responses in Arabidopsis. Plant J **50:** 545–556

Lan P, Li W, Schmidt W (2012) Complementary proteome and transcriptome profiling in phosphate-deficient Arabidopsis roots reveals multiple levels of gene regulation. Mol Cell Proteomics **11:** 1156–1166

Lan P, Li W, Schmidt W (2013) Genome-wide co-expression analysis predicts protein kinases as important regulators of phosphate deficiency-induced root hair remodeling in Arabidopsis. BMC Genomics **14:** 210

Li K, Xu C, Fan W, Zhang H, Hou J, Yang A, Zhang K (2014) Phosphoproteome and proteome analyses reveal low-phosphate mediated plasticity of root developmental and metabolic regulation in maize (*Zea mays* L.). Plant Physiol Biochem **83:** 232–242

Liang C, Tian J, Lam HM, Lim BL, Yan X, Liao H (2010) Biochemical and molecular characterization of PvPAP3, a novel purple acid phosphatase isolated from common bean enhancing extracellular ATP utilization. Plant Physiol **152:** 854–865

Liang CY, Chen ZJ, Yao ZF, Tian J, Liao H (2012) Characterization of two putative protein phosphatase genes and their involvement in phosphorus efficiency in *Phaseolus vulgaris*. J Integr Plant Biol **54:** 400–411

Liu J, Wang X, Huang H, Wang J, Li Z, Wu L, Zhang G, Ma Z (2012) Efficiency of phosphorus utilization in phyA-expressing cotton lines. Indian J Biochem Biophys **49:** 250–256

Liu JQ, Allan DL, Vance CP (2010) Systemic signaling and local sensing of phosphate in common bean: cross-talk between photosynthate and microRNA399. Mol Plant **3:** 428–437

Lung SC, Chan WL, Yip W, Wang L, Yeung EC, Lim BL (2005) Secretion of beta-propeller phytase from tobacco and *Arabidopsis* roots enhances phosphorus utilization. Plant Sci **169:** 341–349

Ma XF, Tudor S, Butler T, Ge Y, Xi Y, Bouton J, Harrison M, Wang ZY (2012) Transgenic expression of phytase and acid phosphatase genes in alfalfa (*Medicago sativa*) leads to improved phosphate uptake in natural soils. Mol Breed **30:** 377–391

Mann DG, Lafayette PR, Abercrombie LL, King ZR, Mazarei M, Halter MC, Poovaiah CR, Baxter H, Shen H, Dixon RA, et al (2012) Gateway-compatible vectors for high-throughput gene functional analysis in switchgrass (*Panicum virgatum* L.) and other monocot species. Plant Biotechnol J **10:** 226–236

Martín AC, del Pozo JC, Iglesias J, Rubio V, Solano R, de La Peña A, Leyva A, Paz-Ares J (2000) Influence of cytokinins on the expression of phosphate starvation responsive genes in *Arabidopsis*. Plant J **24:** 559–567

May A, Berger S, Hertel T, Köck M (2011) The *Arabidopsis thaliana* phosphate starvation responsive gene *AtPPsPase1* encodes a novel type of inorganic pyrophosphatase. Biochim Biophys Acta **1810:** 178–185

May A, Spinka M, Köck M (2012) *Arabidopsis thaliana* PECP1: enzymatic characterization and structural organization of the first plant phosphoethanolamine/phosphocholine phosphatase. Biochim Biophys Acta **1824:** 319–325

Mehra P, Giri J (2016) Rice and chickpea *GDPD*s are preferentially influenced by low phosphate and CaGDPD1 encodes an active glycerophosphodiester phosphodiesterase enzyme. Plant Cell Rep **35:** 1699–1717

Mehra P, Pandey BK, Giri J (2015) Genome-wide DNA polymorphisms in low phosphate tolerant and sensitive rice genotypes. Sci Rep **5:** 13090

Mehra P, Pandey BK, Giri J (2016) Comparative morphophysiological analyses and molecular profiling reveal Pi-efficient strategies of a traditional rice genotype. Front Plant Sci **6:** 1184

Mehra P, Pandey BK, Giri J (2017) Improvement in phosphate acquisition and utilization by a secretory purple acid phosphatase (OsPAP21b) in rice. Plant Biotechnol J http://dx.doi.org/10.1111/pbi.12699

Mikulska M, Bomsel JL, Rychter A (1998) The influence of phosphate deficiency on photosynthesis, respiration and adenine nucleotide pool in bean leaves. Photosynthetica **35:** 79–88

Pant BD, Pant P, Erban A, Huhman D, Kopka J, Scheible WR (2015) Identification of primary and secondary metabolites with phosphorus status-dependent abundance in Arabidopsis, and of the transcription factor PHR1 as a major regulator of metabolic changes during phosphorus limitation. Plant Cell Environ **38:** 172–187

Papademetriou MK (2000) Rice production in the Asia-Pacific region: issues and perspectives. *In* MK Papademetriou, FJ Dent, EM Herath, eds, Bridging the Rice Yield Gap in the Asia-Pacific Region. Food and the Agriculture Organization of the United Nations, Bangkok, Thailand, pp 4–25

Plaxton WC, Shane MW (2015) The role of post-translational enzyme modifications in the metabolic adaptations of phosphorus-deprived plants. Annu Plant Rev **48:** 99–124

Raghothama KG (1999) Phosphate acquisition. Annu Rev Plant Physiol Plant Mol Biol **50:** 665–693

Richardson AE, Hadobas PA, Hayes JE (2001) Extracellular secretion of *Aspergillus* phytase from *Arabidopsis* roots enables plants to obtain phosphorus from phytate. Plant J **25:** 641–649

Ridder IS, Dijkstra BW (1999) Identification of the Mg^{2+}-binding site in the P-type ATPase and phosphatase members of the HAD (haloacid dehalogenase) superfamily by structural similarity to the response regulator protein CheY. Biochem J **15:** 223–226

Singh AP, Pandey BK, Deveshwar P, Narnoliya L, Parida SK, Giri J (2015) JAZ repressors: possible involvement in nutrients deficiency response in rice and chickpea. Front Plant Sci **6:** 975

Singh B, Satyanarayana T (2012) Plant growth promotion by phytases and phytase-producing microbes due to amelioration in phosphorus availability. *In* T Satyanarayana, NB Johri, eds, Microorganisms in Sustainable Agriculture and Biotechnology. Springer, Dordrecht, The Netherlands, pp 3–15

Springer M, Wykoff DD, Miller N, O'Shea EK (2003) Partially phosphorylated Pho4 activates transcription of a subset of phosphate-responsive genes. PLoS Biol **1:** E28

Tilman D, Balzer C, Hill J, Befort BL (2011) Global food demand and the sustainable intensification of agriculture. Proc Natl Acad Sci USA **108:** 20260–20264

Toki S, Hara N, Ono K, Onodera H, Tagiri A, Oka S, Tanaka H (2006) Early infection of scutellum tissue with *Agrobacterium* allows high-speed transformation of rice. Plant J **47:** 969–976

Tran HT, Hurley BA, Plaxton WC (2010a) Feeding hungry plants: the role of purple acid phosphatases in phosphate nutrition. Plant Sci **179:** 14–27

Tran HT, Qian W, Hurley BA, She YM, Wang D, Plaxton WC (2010b) Biochemical and molecular characterization of AtPAP12 and AtPAP26: the predominant purple acid phosphatase isozymes secreted by phosphate-starved *Arabidopsis thaliana*. Plant Cell Environ **33:** 1789–1803

Walter M, Chaban C, Schütze K, Batistic O, Weckermann K, Näke C, Blazevic D, Grefen C, Schumacher K, Oecking C, et al (2004) Visualization of protein interactions in living plant cells using bimolecular fluorescence complementation. Plant J **40:** 428–438

Wang H, Chevalier D, Larue C, Cho SK, Walker JC (2007) The protein phosphatases and protein kinases of Arabidopsis thaliana. The Arabidopsis Book **5:** e0106, doi/10.1199/tab.0106

Wang L, Li Z, Qian W, Guo W, Gao X, Huang L, Wang H, Zhu H, Wu JW, Wang D, et al (2011) The Arabidopsis purple acid phosphatase AtPAP10 is predominantly associated with the root surface and plays an important role in plant tolerance to phosphate limitation. Plant Physiol **157:** 1283–1299

Wang Z, Hu H, Huang H, Duan K, Wu Z, Wu P (2009) Regulation of OsSPX1 and OsSPX3 on expression of OsSPX domain genes and Pi-starvation signaling in rice. J Integr Plant Biol **51:** 663–674

Wissuwa M, Ae N (2001) Genotypic variation for tolerance to phosphorus deficiency in rice and the potential for its exploitation in rice improvement. Plant Breed **120:** 43–48

Wu P, Ma L, Hou X, Wang M, Wu Y, Liu F, Deng XW (2003) Phosphate starvation triggers distinct alterations of genome expression in Arabidopsis roots and leaves. Plant Physiol **132:** 1260–1271

Wu P, Shou H, Xu G, Lian X (2013) Improvement of phosphorus efficiency in rice on the basis of understanding phosphate signaling and homeostasis. Curr Opin Plant Biol **16:** 205–212

Zeng F, Shabala L, Zhou M, Zhang G, Shabala S (2013) Barley responses to combined waterlogging and salinity stress: separating effects of oxygen deprivation and elemental toxicity. Front Plant Sci **4:** 313

Zhang D, Song H, Cheng H, Hao D, Wang H, Kan G, Jin H, Yu D (2014) The acid phosphatase-encoding gene GmACP1 contributes to soybean tolerance to low-phosphorus stress. PLoS Genet **10:** e1004061

Zhou J, Jiao F, Wu Z, Li Y, Wang X, He X, Zhong W, Wu P (2008) OsPHR2 is involved in phosphate-starvation signaling and excessive phosphate accumulation in shoots of plants. Plant Physiol **146:** 1673–1686

Zimmermann P, Zardi G, Lehmann M, Zeder C, Amrhein N, Frossard E, Bucher M (2003) Engineering the root-soil interface via targeted expression of a synthetic phytase gene in trichoblasts. Plant Biotechnol J **1:** 353–360